

RAL-TR-1999-042

TSL/ISV-99-0218

September 1999

Effects of CP-violating phases on Higgs boson production at hadron colliders in the Minimal Supersymmetric Standard Model

A. Dedes¹ and S. Moretti^{1,2}

¹Rutherford Appleton Laboratory,
Chilton, Didcot, Oxon OX11 0QX, UK

²Department of Radiation Sciences, Uppsala University,
P.O. Box 535, 75121 Uppsala, Sweden

Abstract

If the soft Supersymmetry (SUSY) breaking masses and couplings are complex, then the associated CP-violating phases can in principle modify the known phenomenological pattern of the Minimal Supersymmetric Standard Model (MSSM). We investigate here their effects on Higgs boson production in the gluon-gluon fusion mode at the Tevatron and the Large Hadron Collider (LHC), by taking into account all experimental bounds available at present. The by far most stringent ones are those derived from the measurements of the Electric Dipole Moments (EDMs) of fermions. However, it has recently been suggested that, over a sizable portion of the MSSM parameter space, cancellations among the SUSY contributions to the EDMs can take place, so that the CP-violating phases can evade those limits. We find a strong dependence of the production rates of any neutral Higgs state upon the complex masses and couplings over such parts of the MSSM parameter space. We show these effects relatively to the ordinary MSSM rates as well as illustrate them at absolute cross section level at both colliders.

1 Introduction and plan

The soft SUSY breaking parameters of the MSSM can well be complex. Even in the absence of flavour non-conservation in the sfermion sector, the Higgsino mass term, the gaugino masses, the trilinear couplings and the Higgs soft bilinear mass need not be real. Assuming universality of the soft gaugino masses at the Grand Unification (GUT) (or Planck) scale, the effects of complex soft masses and couplings in the MSSM Lagrangian (see Appendix A) can be parametrised in terms of only two independent phases [1], and ϕ_A , associated to the (complex) Higgsino mass term, μ , and to the trilinear scalar coupling A^1 , respectively. In other terms,

$$e^i = \frac{A}{\Lambda_j}; \quad e^{i_A} = \frac{A}{\Lambda_j} : \quad (1)$$

Their presence is a potentially dangerous new source of violation of the CP-symmetry in the MSSM. But their size can in principle strongly be constrained by the measurements of the fermionic EDMs (mainly, of electron and neutron) and several analyses [2] have indicated that μ and ϕ_A must be small in general. However, recent investigations [3, 4] have shown that, in a restricted but still sizable part of the parameter space of the MSSM, the bounds drawn from the EDM measurements are rather weak, so that such phases can even be close to $\pi/2$. This is a consequence of cancellations taking place among the SUSY loop contributions to the EDMs. Although, in order to be effective, these require a certain amount of ‘ne-tuning’ among the soft masses and couplings [4], it has recently been suggested that such cancellations occur naturally in the context of Superstring models [5]. If the SUSY loop contributions to the EDMs do vanish, then, as emphasised by the authors of Ref. [6], SUSY parameters with large imaginary parts may have a non-negligible impact on the confrontation of the MSSM with experiments. In particular, many of the SUSY (s)particle production and decay processes develop a dependence on μ and ϕ_A , so that, in view of the importance of searches for New Physics at present and future accelerators, their phenomenology needs a thorough re-investigation.

Various sparticle processes including the effect of such phases have recently been considered. For example, neutralino [7] and chargino [8] production at LEP, at the CERN LHC [9] as well as at future electron-positron linear colliders (LCs) [10, 11]. Direct CP-asymmetries in decays of heavy hadrons, such as $B \rightarrow X_s + \dots$, $B \rightarrow X_d + \dots$ and $B \rightarrow X_s l^+ l^-$, have been investigated in the context of the Supergravity inspired MSSM (M-SUGRA): in Refs. [12], [13] and [14], respectively.

In this paper, we are concerned with the Higgs sector of the MSSM. Here, although the tree-level Higgs potential is not affected by the CP-violating phases, since $M_{H_1}^2, M_{H_2}^2$ and $\tan \beta$ (the mass parameters of the two Higgs fields and the ratio of their vacuum expectation values (VEVs), respectively) are real and enters only through μ^2 , it should be noticed that this is no longer the case if one includes radiative corrections. In their

¹For simplicity, hereafter (except in the Appendices), we assume $A_u = A_d = A$ at the electroweak (EW) scale, i.e., $O(M_Z)$, where u and d refer to all flavours of up- and down-type (s)quarks.

presence, one finds [15, 16] that the three neutral Higgs bosons can mix and that their effective couplings to fermions can be rather different at one loop. However, for the MSSM parameter space that we will consider here, such corrections turn out to be negligible, of the order of just a few percent, as compared to those induced at the lowest order by the CP-violating phases in the squark sector. There are some reasons for this. First of all, the induced radiative corrections to the Higgs-quark-quark vertices can be parametrised in terms of the mass of the charged Higgs boson, $M_H (\equiv M_{A^\pm})$. Then, one can verify that they essentially depend only upon the input values given to $\tan\beta$, \tilde{A}_j and M_{SUSY} (the typical mass scale of the SUSY partners of ordinary matter). Here, we will mainly be concerned with trilinear couplings in the range $\tilde{A}_j < 700 \text{ GeV}$, Higgsino masses \tilde{m}_j of the order of 600 GeV or so, and $M_{\text{SUSY}} \sim 300 \text{ GeV}$. According to the analytic formulae of Ref. [16], in the above MSSM regime, one finds negligible corrections to the tree-level $h^0 tt$ and $h^0 bb$ couplings. (Similarly, for the case of the lightest Higgs boson mass.) In contrast, the strength of the $H^0 tt$ vertex can significantly be modified for not too heavy masses of the charged Higgs boson (say, $M_H \equiv M_{A^\pm} < 200 \text{ GeV}$) and rather large values of \tilde{A}_j and \tilde{m}_j (typically, $\tilde{A}_j \sim \tilde{m}_j \sim 2 \text{ TeV}$), a region of parameter space that we will avoid, whereas that of the $H^0 bb$ one is generally small because we shall limit ourselves to the interval $2 < \tan\beta < 10$. As for papers allowing instead for the presence of non-zero values of \tilde{m}_j and/or \tilde{A}_j and studying the Higgs sector, one can list Refs. [17] and [18]. The first publications deals with decay rates whereas the second one with Higgs production channels probable at a future LC. In such papers though, no systematic treatment of the limits imposed by the EDM measurements was addressed. Such effects ought to be incorporated in realistic analyses of the MSSM Higgs dynamics.

Here, we have necessarily done so, since it is our purpose to study the effect of finite values of \tilde{m}_j and/or \tilde{A}_j on Higgs production via the $gg \rightarrow h^0$ channel [19], where $h^0 = H^0, h^0$ and A^0 represents any of the three neutral Higgs bosons of the MSSM. (A preliminary account in this respect was already given by the authors in Ref. [20].) These processes proceed through quark (mainly top and bottom: i.e., t and b , see Fig. 1) and squark (mainly stop and sbottom: i.e., \tilde{t}_1, \tilde{t}_2 and \tilde{b}_1, \tilde{b}_2 , see Fig. 2, each in increasing order of mass) loops, in which the (s)fermions couple directly to h^0 . Needless to say, as in the MSSM the lightest of the Higgs particles is bound to have a mass not much larger than that of the Z boson, M_Z , much of the experimental effort at both the Tevatron (Run 2) and the LHC will be focused on finding this Higgs state, h^0 . In this respect, we remind the reader that direct Higgs production via gluon-gluon fusion is the dominant mechanism over a large portion of the MSSM parameter space at the LHC and a sizable one at the Tevatron [21].

The plan of the paper is as follows. The next Section describes our theoretical framework and discusses experimental limits on the parameters of the model. The following one briefly sketches the way we have performed the calculation. Sect. 4 presents some numerical results, whereas Sect. 5 summarises our analysis and draws the conclusions. Finally, in the two Appendices, we introduce our notation and explicitly derive the Feynman rules and cross section formulae needed for our numerical analysis.

2 The theoretical model and its parameters

We work in the theoretical framework provided by the MSSM, the latter including explicitly the CP-violating phases and assuming universality of the soft gaugino masses at the GUT scale and universality of the soft trilinear couplings at the EW scale. We define its parameters at the EW scale, without making any assumptions about the structure of the SUSY breaking dynamics at the Planck scale, whether driven by Supergravity (SUGRA), gauge mediated (GMSB) or proceeding via other (yet unknown) mechanisms. We treat the MSSM as a low-energy effective theory, and input all parameters needed for our analysis independently from each other. However, we require these to be consistent with current experimental bounds. In fact, given the dramatic impact that the latter can have on the viability at the Tevatron and/or the LHC of the CP-violating effects in the processes we are dealing with, we specifically devote the two following Subsections to discuss all available experimental constraints. The first focuses on collider data, from LEP and Tevatron; the second on the measurements of the fermionic EDMs. (Some bounds can also be derived from the requirement of positive definiteness of the squark masses squared.) Following this discussion, we will establish the currently allowed ranges for the Higgs and sparticle masses and couplings.

Before proceeding in this respect though, we declare the numerical values adopted for those MSSM parameters that are in common with the Standard Model (SM). For the top and bottom masses entering the SM-like fermionic loops of our process, we have used $m_t = 175 \text{ GeV}$ and $m_b = 4.9 \text{ GeV}$, respectively. As for the gauge couplings, the strong, electromagnetic (EM) coupling constants and the sine squared of the Weinberg angle, we have adopted the following values: $\alpha_s(M_Z) = 0.119$, $\alpha_{EM}(M_Z) = 1/127.9$ and $\sin^2 \theta_W(M_Z) = 0.2315$, respectively.

2.1 Limits from colliders

The Higgs bosons and sparticles of the MSSM that enter the $gg \rightarrow \gamma\gamma$ production processes can also be produced via other channels, both as real and virtual objects. From their search at past and present colliders, several limits on their masses and couplings have been drawn. As for the neutral Higgs bosons of the MSSM, the most stringent bounds come from LEP. For both M_{h^0} and M_{A^0} these are set { after the 1998 LEP runs { at around 80 GeV by all Collaborations [22], for $\tan \beta > 1^2$. The tightest experimental limits on the squark masses come from direct searches at the Tevatron. Concerning the \tilde{t}_1 mass, for the upper value of $\tan \beta$ that we will be using here, i.e., 10, the limit on $m_{\tilde{t}_1}$ can safely be drawn at 120 GeV or so [24], fairly independently of the SUSY model assumed. As for the lightest sbottom mass, $m_{\tilde{b}_1}$, this is excluded for somewhat lower values, see

²See also [23] for a more recent and somewhat higher limit { that we adopt here { on M_{h^0} from ALEPH, of about 85.2 GeV for $\tan \beta = 1$ at 95% confidence level (CL), using data collected at collider centre-of-mass (CM) energies in the range $192 \text{ GeV} < \sqrt{s_{ee}} < 196 \text{ GeV}$ and a total luminosity of about 100 pb^{-1} .

Ref. [25]. Besides, D also contradicts all models with $m_{\tilde{q}\tilde{t}_1\tilde{b}_1} < 250 \text{ GeV}$ for $\tan\beta < 2$, $A = 0$ and $\mu < 0$ [26] (in scenarios with equal squark and gluino masses the limit goes up to $m_{\tilde{q}\tilde{t}_1\tilde{b}_1} < 260 \text{ GeV}$).

2.2 Limits from the EDMs

These are possibly the most stringent experimental constraints available at present on the size of the CP-violating phases. The name itself owes much to the consequences induced in the QED sector. In fact, to introduce a complex part into the soft SUSY breaking parameters of the MSSM corresponds to ‘explicitly’ violating CP-invariance in the matrix elements (MEs) involving the EM current, as the phases lead to non-zero TP form factors, which in turn contribute to the fermionic EDMs. In contrast, within the SM, it is well known that contributions to the EDMs arise only from higher-order CP-violating effects in the quark sector, and they are much smaller than the current experimental upper bounds. At 90% CL, those on the electron, d_e [27], and neutron, d_n [28], read as:

$$|d_{e,n}|_{\text{exp}} \leq 4.3 \cdot 10^{27} \text{ e cm} ; \quad |d_{e,n}|_{\text{exp}} \leq 6.3 \cdot 10^{26} \text{ e cm} ; \quad (2)$$

As mentioned in the Introduction, if cancellations take place among the SUSY contributions to the electron and neutron EDMs, so that their value in the MSSM is well below the above limits, i.e., $|d_{e,n}|_{\text{MSSM}} \ll |d_{e,n}|_{\text{exp}}$ and $|d_{e,n}|_{\text{MSSM}} \ll |d_{e,n}|_{\text{exp}}$, then μ and A can be large. To search for those combinations of soft sparticle masses and couplings that guarantee vanishing SUSY contributions to the EDMs for each possible choice of the CP-violating phases, we have scanned over the $(\mu; A)$ plane and made use of the program of Ref. [4]. This returns those minimum values of the modulus of the common trilinear coupling, \tilde{A}_j , above which the cancellations work. For instance, in the case of the neutron EDMs, the dominant chargino and gluino contributions appear with opposite sign over a large portion of the MSSM parameter space. Thus, for a given j , a chargino diagram can cancel a gluino one and this occurs for certain values of the gaugino/squark masses and a specific choice of \tilde{A}_j [3, 4]. In general, internal cancellations are more likely among the SUSY contributions to the neutron EDMs, than they are in the case of the electron. So much so that, in the former case, it is even possible to remain consistently above the experimental limits (2) if one only assumes the phase of j to be non-zero [4].

However, not all the surviving combinations of μ , A and \tilde{A}_j are necessarily allowed. In fact, one should recall that physical parameters of the MSSM depend upon these three inputs. In particular, the squark masses (entering the triangle loops of the production processes considered here) are strongly related to μ , A and \tilde{A}_j . Given the assumptions already made on the trilinear couplings (i.e., their universality), and further setting (see Appendix A for the notation)

$$M_{\tilde{g}} = M_{\tilde{Q}_3} = M_{\tilde{U}_3} = M_{\tilde{D}_3} ; \quad (3)$$

$$M_{\tilde{q}_{1,2}} = M_{\tilde{Q}_{1,2}} = M_{\tilde{U}_{1,2}} = M_{\tilde{D}_{1,2}} ; \quad (4)$$

with $M_{\tilde{q}_{1,2}} > M_{\tilde{q}_3}$, where $M_{\tilde{q}_{1,2,3}}$ are the soft squark masses of the three generations, one gets for the lightest stop and sbottom masses the following relations:

$$m_{\tilde{t}_1}^2 = \frac{M_{\tilde{q}_3}^2 + m_t^2 + \frac{1}{4}M_Z^2 \cos 2\beta}{r} - \frac{h}{t} \frac{(-\frac{5}{6}M_Z^2 - \frac{4}{3}M_W^2)^2 \cos^2 2\beta + 4m_t^2 \tilde{A}^2 + j^2 \cot^2 + 2\tilde{A}jj \cos(\beta_A) \cot \beta}{t}; \quad (5)$$

$$m_{\tilde{b}_1}^2 = \frac{M_{\tilde{q}_3}^2 + m_b^2 + \frac{1}{4}M_Z^2 \cos 2\beta}{r} - \frac{h}{t} \frac{(\frac{1}{6}M_Z^2 - \frac{2}{3}M_W^2)^2 \cos^2 2\beta + 4m_b^2 \tilde{A}^2 + j^2 \tan^2 + 2\tilde{A}jj \cos(\beta_A) \tan \beta}{t}; \quad (6)$$

For some choices of β , β_A and \tilde{A} and a given value of $M_{\tilde{q}_3}$, j and $\tan \beta$, the two above masses (squared) can become negative. This leads to a breaking of the $SU(3)$ symmetry, that is, to the appearance of colour and charge breaking minima. In order to avoid this, some points on the plane $(\beta; \beta_A)$ will further be excluded in our study.

3 Numerical calculation

We have calculated the Higgs production rates in presence of the CP-violating phases exactly at the leading order (LO) and compared them to the yield of the ordinary MSSM (that is, 'phaseless') at the same accuracy. In our simulations, we have included only the t -, b -, \tilde{t}_1 -, \tilde{t}_2 -, \tilde{b}_1 - and \tilde{b}_2 -loops, indeed the dominant terms, because of the Yukawa type couplings involved. In order to do so, we had to compute from scratch all the relevant analytical formulae for A^0 production. In fact, one should notice that for such a Higgs state there exist no tree-level couplings with identical squarks if $\beta = \beta_A = 0$, whereas they appear at lowest order whenever one of these two parameters is non-zero. Besides, being the quark loop contributions antisymmetric (recall that A^0 is a pseudoscalar state) and the squark loop ones symmetric, no interference effects can take place between the SM- and the SUSY-like terms in the ME for $gg \rightarrow A^0$. (That is to say that β - and β_A -induced corrections are always positive if $\beta^0 = A^0$.) The full amplitude is given explicitly in Appendix B. For completeness, we have also recomputed the wellknown expressions for scalar Higgs production, $\beta^0 = h^0; H^0$, finding perfect agreement with those already given in literature (again, see Appendix B). Here, CP-violating effects can produce corrections of both signs.

It is well known that next-to-leading order (NLO) corrections to $gg \rightarrow \beta^0$ processes from ordinary QCD are very large [29, 30]. However, it has been shown that they affect the quark and squark contributions very similarly [30]. Thus, as a preliminary exercise, one can look at the LO rates only in order to estimate the effects induced by the CP-violating phases. In contrast, for more phenomenological analyses, one ought to incorporate these

QCD effects. We have eventually done so by resorting to the analytical expressions for the heavy (s)quark limit given in Ref. [30]. These are expected to be a very good approximation for Higgs masses below the quark-quark and squark-squark thresholds. Therefore, we will confine ourselves to combinations of masses which respect such kinematic condition.

As Parton Distribution Functions (PDFs), we have used the sets MR98-LQ (05A) [31] and MR98-NLO (ET08) [32], in correspondence of our one- and two-loop simulations, respectively. Consistently, we have adopted the one- and two-loop expansion for the strong coupling constant $\alpha_s(Q)$, with all relevant (s)particle thresholds onset within the MSSM as described in [33]. The running of the latter, as well as the evolution of the PDFs, was always described in terms of the factorisation scale $Q = Q_F$, which was set equal to the produced Higgs mass, M_{H^0} . In fact, the same value was adopted for the renormalisation scale $Q = Q_R$ entering the Higgs production processes, see eqs. (B.1) and (B.6)–(B.7).

Finally, for CM energy of the LHC, we have assumed $\sqrt{s_{pp}} = 14 \text{ TeV}$; whereas for the Tevatron, we have taken $\sqrt{s_{pp}} = 2 \text{ TeV}$.

4 Results

A sample of μ , A_0 and \tilde{A}_j values that guarantee the mentioned cancellations can be found in Fig. 3, for the two representative choices of $M_{\tilde{g},2}$ given in Tab. I. Here, both \tilde{m}_j and $M_{\tilde{g}}$ are held constant at, e.g., 600 and 300 GeV, respectively. The soft gluino mass is given too, in Tab. I, as it enters our analysis indirectly, through the EDM constraints (recall the discussion in Subsect. 2.2). The allowed values for the modulus of the (common) trilinear couplings \tilde{A}_j are displayed in the form of a contour plot over the $(\mu; A_0)$ plane, where both phases are varied from 0 to 2π . (Same results are obtained in the interval $(-2\pi; 2\pi)$, because of the periodic form of the SUSY couplings and mixing angles: see Appendix A.) In the same plots, we have superimposed those regions (to be excluded from further consideration) over which the observable MSSM parameters assume values that are either forbidden by collider limits (dots for the lightest stop mass and squares for the lightest Higgs mass: see Figs. 4(5 below) or for which the squark masses squared become negative (crosses), for a given combination of the other soft SUSY breaking parameters. Typically, we obtain that for small phases, i.e., $\mu < 300$ GeV, the value of \tilde{A}_j tends to be zero for almost all values of A_0 . In the region where both phases are quite large ($\mu; A_0 \approx 2\pi$), the modulus of the trilinear coupling must be around 700 GeV, for the EDM constraints to be satisfied.

In Tab. I, in order to completely define our model for the calculation of the $gg \rightarrow H^0$ processes, we also have introduced the Higgs sector parameters: the mass of one physical states, e.g., M_{A^0} , and the ratio of the VEVs of the two doublet fields, i.e., $\tan \beta$. We have fixed the former to be 200 GeV, whereas two possible choices of the latter have been adopted, 2.7 and 10 (corresponding to $M_{\tilde{g},2} = 1000$ and 300 GeV, respectively). With regard to this last parameter, $\tan \beta$, a few considerations have to be made at this

point: namely, concerning the so-called ‘Barr-Zee type graphs’ [34]. Very recently, the corresponding contributions to the electron and neutron EDMs have been calculated at two loops, in Ref. [35]. These terms put bounds (diamond symbols) directly on the squark masses and soft trilinear couplings of the third generation and thus are crucial for our analysis. However, they are quantitatively significant only at large values of $\tan\beta$, as can be appreciated in the right-hand plot of Fig. 3. The smaller $\tan\beta$ the less relevant they are: see the left-hand plot of the same figure. Besides, these two-loop terms entering the EDMs also depend on j_j : small values of the latter induce negligible contributions to both the electron and neutron EDMs. (For example, for the choice $j_j = 500$ GeV and $\tan\beta = 3$ made in Ref. [20], one obtains no bounds from the EDMs through the Barr-Zee type graphs.) Moreover, for $\tan\beta > 10$, in order to be consistent with the EDM constraints in (2), one would need the modulus of the soft trilinear coupling to be unnaturally large, even greater than 4 TeV (for $A_0 = 2$). This would drive the squark masses in eqs. (5)–(6) to become negative over most of the (μ, A) plane. Thus, in order to avoid all such effects, we limit our analysis to the interval $2 < \tan\beta < 10$ (recall the lower experimental limit on such a parameter: see Subsect. 2.1). Corresponding values for the modulus of the (common) trilinear couplings are in the range $|A_j| < 1$ TeV. In this regime, the parameter combinations given in Tab. I should serve the sole purpose of being examples of the rich phenomenology that can be induced by the CP-violating phases in the MSSM, rather than benchmark cases.

$\tan\beta$	j_j	$M_{\tilde{u}_{1,2}}$	$M_{\tilde{u}_3}$	$M_{\tilde{g}}$	M_{A^0}
2.7	600	1000	300	300	200
10	600	300	300	300	200

Table I: Two possible parameters setups of our model. (Apart from the dimensionless $\tan\beta$, all other quantities are given in GeV.)

Furthermore, notice that, starting from the numbers in Tab. I, one can verify that the heaviest squark masses, $m_{\tilde{t}_2}$ and $m_{\tilde{b}_2}$, are both consistent with current experimental bounds. As for the lightest stop, we display in Fig. 4 the values assumed by $m_{\tilde{t}_1}$ over the usual $(\mu; A)$ plane, for the two choices of $\tan\beta$ in Tab. I and in correspondence of the j_j values of the previous figure. As a matter of fact, the effect of the phases is quite significant on the actual lightest stop mass, see eq. (5). We observe that, for $\tan\beta = 2.7$, one can get small values for $m_{\tilde{t}_1}$, if not negative. This is due to the fact that, in such a region, $|A_j|$ can still get large enough (despite of a low $\tan\beta$), so that the last term on the right-hand side of eq. (5) becomes comparable to the first two terms. Anyhow, over most of the $(\mu; A)$ plane, $m_{\tilde{t}_1}$ is well above the current experimental reach of 120 GeV. The lightest sbottom mass, $m_{\tilde{b}_1}$, see eq. (6), is always around 290 GeV, so that we have avoided to reproduce here the corresponding plots. Also, for the above choices of $\tan\beta$, one gets constraints on the mass of the lightest Higgs boson. In order to derive these, we make use of the two-loop analytic formula for M_{h^0} [36]. We display the corresponding values over the $(\mu; A)$ plane in Fig. 5. The mass regions excluded by LEP (see Subsect. 2.1) amount

to a restricted part of the $(\beta; A)$ plane, both at small and, particularly, large $\tan\beta$. As for the heaviest Higgs boson masses, one has $M_{H^0} = 212(201)$ GeV for $\tan\beta = 2:7(10)$, thus almost degenerate with M_{A^0} .

Having defined the allowed spectrum for the (s)particle masses and couplings entering the Higgs production modes that we are considering, we are now ready to quantify the effects of the phases on the actual cross sections. A convenient way of doing so is to simply look at the ratio between the MEs computed with and without phases. In fact, at LO accuracy and further assuming that the relevant hard scale is the same in both cases (e.g., $Q = M_{H^0}$), such a ratio coincides with that obtained at cross section level, independently of the choice of the PDFs and of \sqrt{s} . Thus, we define

$$R(gg \rightarrow H^0) = \frac{M_{LO}^{SSM}(gg \rightarrow H^0)}{M_{LO}^{SSM}(gg \rightarrow H^0)} : \quad (7)$$

By means of the notation M_{LO}^{SSM} , we refer here and in the following to the case of the MSSM with same β but finite values of either α or A . Thus, e.g., when $\alpha = A = 0$ (and $\beta = 0$ too, see Fig. 3), the expression in (7) is of course equal to 1. (Several results for this ratio have already been presented in Ref. [20], though for a choice of the MSSM parameters different from those considered here.)

In Fig. 6 we present $R(gg \rightarrow h^0)$ as a contour plot over the $(\beta; A)$ plane for the two choices of MSSM parameters of Tab. I. As a consequence of the expression for the $gg \rightarrow h^0$ amplitude, see eq. (B.1), the corrections induced by the presence of finite values of α and/or A in the squark loops can be either positive or negative. Interestingly enough, destructive interferences take place over regions already excluded by direct Higgs searches. Only constructive interferences would then be observable. These can considerably enhance the value of the cross sections obtained in the ordinary MSSM, particularly at large A and intermediate α values, if $\tan\beta$ is small (by up to a factor of 7). This result is a consequence of two related aspects. Firstly, in those $(\beta; A)$ regions, β achieves its maximum, so that the corresponding Higgs-squark-squark couplings are enhanced significantly, with respect to the strength of the Higgs-quark-quark vertices (see Appendix A). Secondly, large values of β correspond to small values of $m_{\tilde{t}_1}$ (compare Fig. 3 to Fig. 4), this yielding a further kinematic enhancement in the squark loops. For large $\tan\beta$, the portion of the $(\beta; A)$ plane surviving the EDM constraints is much smaller, but the CP-violating effects are still large. For example, in the region $3 = 5 < \alpha < 3 = 4$ and $-3 < A < 3 = 4$, the MSSM cross sections can be larger by about a factor of 5 with respect to the MSSM ones.

In Fig. 7 we present similar rates for the heaviest scalar Higgs boson, i.e., $H^0 = H^0$. Contrary to the previous case, here, one typically obtains a suppression of the MSSM cross sections relatively to the MSSM ones, over the allowed regions of the $(\beta; A)$ plane, both at small and large $\tan\beta$. The destructive effect is the consequence of the interplay between the Higgs mixing angle α and the minus sign in the third term of the relevant $H^0 \tilde{t}_1 \tilde{t}_1$ coupling, see eq. (A.49), as opposed to a plus sign in $h^0 \tilde{t}_1 \tilde{t}_1$ of eq. (A.53). Quantitatively, the effects of the phases are most conspicuous at small $\tan\beta$, when $\alpha \approx \beta$.

$3 \approx 5$ for small A values (about one order of magnitude difference between the MSSM and the MSSM, at the most). At large $\tan\beta$, over the much smaller $(\beta; A)$ plane surviving the experimental constraints, the suppression is at most a factor of 2, when $\beta \approx 4 \approx 5$.

The ratio $R(gg \rightarrow A^0)$ is plotted in Fig. 8. As already discussed in Sect. 3, here the corrections induced by finite values of β and/or A are always positive: see eq. (B.1). In fact, the ratio $R(gg \rightarrow A^0)$ can become as large as 2 at small $\tan\beta$. In this case, the maximum is obtained very close to the excluded regions: i.e., $\beta \approx 2$ and $A \approx 0$. This pattern can easily be understood by looking at the $A^0 \bar{t}_1 t_1$ coupling of eq. (A.48) and further recalling eq. (A.20). (Also notice that, for $A = \beta/2$ and $\tan\beta = 2/7$, the coupling $A^0 \bar{t}_1 t_1$ becomes zero, hence $R(gg \rightarrow A^0) = 1$.) For larger values of $\tan\beta$, the effects of the phases on pseudoscalar Higgs boson production can even be larger, as they are induced through the $A^0 \bar{b}_1 b_1$ vertex of eq. (A.48), which benefits from the $\tan\beta$ enhancement. For example, when $\beta \approx 3 \approx 4$ and for A slightly larger than $\beta/2$, the increase can amount to a factor of 3.

As general remark on the behaviour of the three ratios, one should notice that they are close to unity (i.e., no effects from the CP-violating phases) when β is small for every value of A . This can easily be interpreted by looking at Fig. 3, since, when $\beta \rightarrow 0$, one has that $\beta_j \rightarrow 0$ and $\bar{t}_j \rightarrow 0$ too (these are the mixing angles of the third generation, see Appendix A). Thus, the strength of all Higgs-squark-squark vertices becomes very small compared to that of the Higgs-quark-quark ones. The opposite ($\beta_j \rightarrow 0$ when $A \rightarrow 0$ for any j) is not true, since here the j value is fixed and thus \bar{t}_j are always non-zero.

As already intimated in Sect. 3, in order to give realistic predictions for CP-violating effects in $gg \rightarrow A^0$ processes, one ought to include two-loop QCD effects. We do so in the remainder of this Section, by considering the NLO production rates of all Higgs states at the mentioned CERN and FNAL colliders, $\frac{M_{\text{SSM}}}{M_{\text{NLO}}}(gg \rightarrow A^0)$. We convert the total production cross sections to picobarns and again adopt the input parameters of Tab. I. (Incidentally, notice that, being $m_{\bar{t}_1} > 120$ GeV, the relation $M_0 < 2m_{\bar{q}}$ is always satisfied, for any $\bar{q} = \bar{t}_1; \bar{t}_2; \bar{b}_1; \bar{b}_2$: recall the discussion in Sect. 3.) The LHC rates are displayed through Figs. 9{11 whereas the Tevatron ones appear in Figs. 12{14. We present these figures mainly as a reference for experimental analyses. In fact, as far as CP-violating effects are concerned, the two-loop QCD dynamics is very similar to the one-loop one already discussed. In particular, we have verified that the QCD K -factors for the quark and squark loops are very similar [30] over the portions of the MSSM parameter space considered here. Thus, to obtain the effects of β and A on Higgs production via gluon-gluon fusion at NLO, it suffices to refer to Figs. 6{8 with the normalisation of Figs. 9{11 and Figs. 12{14, for the LHC and the Tevatron, respectively. Concerning the possibility of actually observing the CP-violating effects at either collider, this is very much dependent upon their luminosities.

At the LHC, with an annual value between 10 and 100 fb⁻¹, all the available $(\beta; A)$ areas can in principle be covered, at both large and small $\tan\beta$ and for all Higgs states, as the production cross sections are never smaller than 5 pb or so, see Figs. 9{11. In particular, this is true where the effects of β and A are larger: compare the areas

with high $R(gg \rightarrow \phi^0)$ values in Figs. 6{8 to the corresponding rates in Figs. 9{11. For example, for $\phi^0 = h^0$, at large A , intermediate $\tan\beta$ and for $\tan\beta = 2:7$, $\sigma_{\text{NLO}}^{\text{MSSM}}(gg \rightarrow h^0)$ is around 200 pb. At large $\tan\beta$, when $3 = 5 < \tan\beta < 3 = 4$ and $3 = 3 < \tan\beta < 3 = 4$, the MSSM cross sections are around 100 pb or more. Similarly, for $\phi^0 = H^0$, if $\tan\beta = 2:7$, when $\tan\beta = 3 = 5$ and for small A values, $\sigma_{\text{NLO}}^{\text{MSSM}}(gg \rightarrow H^0)$ is of the order of 6 pb. At $\tan\beta = 10$, when $\tan\beta = 4 = 5$ (for any A), one gets cross section rates around 10 pb. Finally, if $\phi^0 = A^0$, at small $\tan\beta$ and when $\tan\beta = 2$ with $A = 0$; , one has again MSSM cross sections of the order of 10 pb. For large $\tan\beta$, $\tan\beta = 3 = 4$ and $A > 2$, $\sigma_{\text{NLO}}^{\text{MSSM}}(gg \rightarrow A^0)$ is about 15 pb.

Concerning the Tevatron, given the value of integrated luminosity expected at Run 2, of the order of 10 fb^{-1} , prospects of detecting CP-violating effects in $gg \rightarrow \phi^0$ processes are very slim. The various $\sigma_{\text{NLO}}^{\text{MSSM}}(gg \rightarrow \phi^0)$'s are notably smaller here, because of the reduced gluon content inside the (anti)proton at lower \sqrt{s} , for a given M_ϕ value. In fact, the production rates over not yet excluded $(\tan\beta; A)$ regions are never larger than a handful of picobarns. One can possibly aim at disentangling CP-violating effects in the case of the lightest Higgs boson, at both $\tan\beta$'s, but only in the usual corners where both the corrections and the absolute production rates are largest: see Fig. 12. As for the other two Higgs states, the chances are extremely poor, as $\sigma_{\text{NLO}}^{\text{MSSM}}(gg \rightarrow \phi^0)$ is always well below the picobarn level, see Figs. 13{14.

As a final remark of this Section, we would like to mention the following. A peculiar feature concerning Figs. 9{10, as compared to Figs. 6{7, respectively, is the different pattern of the level curves. This should not be surprising though, as, for $\phi^0 = h^0; H^0$, the squark loop contributions in the ordinary MSSM are non-zero to start with. In contrast, one can appreciate the strong correlations between the level curves in Fig. 11 and Fig. 6, a consequence of the absence of scalar loops in $gg \rightarrow A^0$ if $\tan\beta = A = 0$. Similarly, for the case of Figs. 12{14.

5 Summary and conclusions

It is well known that finite values of the mixing angles $\tan\beta$, converting the weak into the mass basis of the third generation of squarks, see eqs. (A.6) and (A.9), imply that left-right chiral currents, eqs. (A.26){(A.37), can enter the Higgs-squark-squark couplings appearing in the scalar loops contributing to $gg \rightarrow \phi^0$ processes, if $\phi^0 = h^0; H^0$, because of the structure of the mixing equations (A.15). As a consequence, the corresponding ϕ^0 production cross sections develop a dependence on $\tan\beta$ and A , the Higgsino mass term and the trilinear scalar coupling (the latter assumed here to be universal to all (s)quark flavours) entering the soft SUSY breaking sector. The strength of their contribution is however modified if CP-violating effects are manifestly inserted into the MSSM Lagrangian, by allowing these two parameters to be complex, see eqs. (A.48){(A.56). In such a case, in particular, also the $gg \rightarrow A^0$ cross section receives scalar loop contributions, thus acquiring a dependence upon $\tan\beta$ and A , much on the same footing as when $\phi^0 = h^0; H^0$: see eq. (B.1).

Clearly, it is the actual size of the independent phases associated to the above two parameters, ϕ and ϕ_A , that regulates the phenomenological impact of complex values of μ and/or A , not least, because they also affect the two mixing angles: see eqs. (A.19) and (A.24). Given the importance of Higgs production at future hadron-hadron colliders, such as the Tevatron (Run 2) and the LHC, and the fact that gluon-gluon fusion is a sizable production mode at the former and indeed the dominant one at the latter (over most of the MSSM parameter space), we have made the investigation of the effects induced by finite CP-violating phases in $gg \rightarrow \gamma\gamma$ processes the concern of this paper. In order to address the problem quantitatively, we first had to derive the relevant Feynman rules of the MSSM in presence of μ and A (Appendix A) and eventually calculate the associated cross sections, for any Higgs state (Appendix B).

Before proceeding to the numerical analysis though, we had to introduce a parametrisation of our theoretical model and incorporate the latest experimental constraints on its parameters. These can be subdivided into two categories, those arising from analyses performed with collider data and those deduced from the measurements of the electron and neutron EDMs. The former mainly limit the value of the squark masses and couplings, thus only indirectly affecting μ and A , see eqs. (5)-(6). In contrast, the latter can be very stringent in this respect, unless cancellations take place among the SUSY contributions to the fermionic EDMs, so that the bounds derived this way on μ and A become much less potent. In practice, the CP-violating phases can attain any value between 0 and 2π , provided j_L and j_R are in appropriate relations, which are in fact satisfied over large portions of the MSSM parameter space. Under these circumstances then, the CP-violating phases can affect the interplay between the quark and squark loops in $gg \rightarrow \gamma\gamma$ processes considerably (Section 2).

In the end, we have verified, both at LO and NLO accuracy (Section 3), that this is true, over those parts of MSSM parameter space where these cancellations are more effective. As a matter of fact, effects due to finite values of μ and/or A can be extremely large, inducing variations on the Higgs cross sections of the ordinary MSSM (i.e., those obtained for $\mu = A = 0$ at the same $\tan\beta$) of several hundred percent, at least for values of $\tan\beta$ in the range between 2 and 10 and soft masses and couplings below the TeV region (Section 4). For these combinations of parameters, even the bounds induced by the contributions of the Barr-Zee type diagrams to the EDMs can easily be evaded. Other than studying relative effects of the phases, with respect to the yield of the ordinary MSSM, we also have presented absolute rates for the $gg \rightarrow \gamma\gamma$ cross sections at NLO, at both the LHC and the Tevatron, for the MSSM including μ and A , thus showing CP-violating effects explicitly in observable quantities. Given the higher luminosity and production rates expected at the CERN collider, as compared to the values at the FNAL one, real prospects of sizing these effects in Higgs boson production will most likely have to wait for a few more years. By then, the available portions of the $(\mu; A)$ plane should also be expected to be better defined than at present, given the improvement foreseen in the near future in the precision of the EDM measurements [37].

Anyhow, as we have tried to motivate in the Introduction, and following our results,

we believe that further investigation is needed of the consequences of explicit CP-violation being present in the soft SUSY Lagrangian. For example, to stay with the Higgs sector, one should establish the effects of μ and A_0 in the decay process $h^0 \rightarrow \dots$ [39], as this represents the most promising discovery channel of the lightest Higgs boson of the MSSM at hadron-hadron machines. In this case, the proliferation of SUSY induced contributions (also due to charged Higgs bosons, sleptons and gauginos) could well be responsible of CP-violating effects comparable to those seen in the Higgs production processes via gluon-gluon fusion, as the latter are solely due to squarks contributions.

Acknowledgements

S.M. acknowledges financial support from the UK PPARC and A.D. that from the Marie Curie Research Training Grant ERB-FMBICT 98-3438. We thank J. Rosiek for providing us with his computer program and for his assistance in using it. A.D. would also like to thank Dick Roberts, Mike Seymour and Apostolos Pilaftsis for helpful discussions.

References

- [1] M. Dugan, B. Grinstein and L. Hall, Nucl. Phys. B 255 (1985) 413; S. Dimopoulos and S. Thomas, Nucl. Phys. B 465 (1996) 23.
- [2] For some reviews, see, e.g.:
 W. Bernreuther and M. Suzuki, Rev. Mod. Phys. 63 (313) 1991; A. Masiero and L. Silvestrini, lecture given at the 'International School on Subnuclear Physics, 35th Course', Erice, Italy, 26 August-4 September 1997 and at the 'International School of Physics Enrico Fermi, Course CXXV II', Varenna, Italy, 8-18 July 1997, preprint TUM-HEP-303/97, December 1997, hep-ph/9711401; Y. Grossman, Y. Nir and R. Rattazzi, preprint SLAC-PUB-7379, WIS-96/49/Dec-PH, CERN-TH/96-368, to appear in the Review Volume 'Heavy Flavours II', eds. A.J. Buras and M. Lindner, Advanced Series on Directions in High Energy Physics, World Scientific Publishing Co., Singapore, April 1997, hep-ph/9701231.
- [3] T. Ibrahim and P. Nath, Phys. Rev. D 57 (1998) 478; T. Falk and K.A. Olive, Phys. Lett. B 439 (1998) 71; W. Hollik, J.I. Illana, S. Rigolin, C. Schappacher and D. Stockinger, Nucl. Phys. B 551 (1999) 3; T. Falk, A. Ferstl and K.A. Olive, Phys. Rev. D 59 (1999) 055009; T. Ibrahim and P. Nath, Phys. Rev. D 58 (1998) 111301; M. Břhlik, G.J. Good and G.L. Kane, Phys. Rev. D 59 (1999) 115004; A. Bartl, T. Gajdosik, W. Porod, P. Stockinger and H. Stremnitzer, preprint UW ThPh{ 1998{63, HEPHY{PUB 705, March 1999, hep-ph/9903402; T. Falk, K.A. Olive, M. Pospelov and R. Roiban, preprint UMN{TH{1757/99, MADPH-99-1113, April 1999, hep-ph/9904393.

- [4] S. Pokorski, J. Rosiek and C.A. Savoy, preprint IFT/99/10, July 1999, hep-ph/9906206.
- [5] M. Brhlik, L. Everett, G.L. Kane and J. Lykken, preprint FERMILAB-Pub-99/136-T, August 1999, hep-ph/9905215; preprint FERMILAB-PUB-99/230-T, August 1999, hep-ph/9908326; E. Accomando, R. Amositt and B. Dutta, preprint CTP-TAMU-34-99, September 1999, hep-ph/9909333.
- [6] M. Brhlik and G.L. Kane, Phys. Lett. B 437 (1998) 331.
- [7] S.Y. Choi, H.S. Song and W.Y. Song, preprint KIAS-P 99057, MADPH-99-1130, SNUTP 99-035, July 1999, hep-ph/9907474; T. Falk, A. Ferstl and K.A. Olive, preprint UMN-TH-1811/99, TPIMINN-99/36, MADPH-99-1125, August 1999, hep-ph/9908311; J.-L. Kneur and G. Moutaka, preprint PM/99-30, July 1999, hep-ph/9907360.
- [8] S.Y. Choi, A. Djouadi, H. Dreiner, J. Kalinowski and P.M. Zerwas, Eur. Phys. J. C 7 (1999) 123; S.Y. Choi, A. Djouadi, H.S. Song and P.M. Zerwas, Eur. Phys. J. C 8 (1999) 669.
- [9] W.-G. Ma, F. Du, M.-L. Zhou, Y. Jiang, L. Han and H. Zhou, preprint July 1999, hep-ph/9907368.
- [10] M.-L. Zhou, W.-G. Ma, L. Han, Y. Jiang and H. Zhou, preprint March 1999, hep-ph/9903376.
- [11] V. Barger, T. Han, T. Li and T. Plehn, preprint MADPH-99-1128, August 1999, hep-ph/9907425.
- [12] T. Goto, Y.Y. Keum, T. Nihei, Y. Okada and Y. Shimizu, Phys. Lett. B 460 (1999) 333; M. Aoki, G.-C. Cho and N. Oshimo, Nucl. Phys. B 554 (1999) 50.
- [13] H.H. Asatrian and H.M. Asatrian, Phys. Lett. B 460 (1999) 148.
- [14] S. Baek and P. Ko, preprint KAIST-TH 99/1, April 1999, hep-ph/9904283; C.-S. Huang and L. Wei, preprint August 1999, hep-ph/9908246.
- [15] D.A. Demir, Phys. Rev. D 60 (1999) 055006; preprint IC/99/62, May 1999, hep-ph/9905571.
- [16] A. Pilaftsis, Phys. Lett. B 435 (1998) 88; Phys. Rev. D 58 (1998) 096010; A. Pilaftsis and C.E. Wagner, Nucl. Phys. B 553 (1999) 3.
- [17] K.S. Babu, C. Kolda, J. March-Russell and F. Wilczek, Phys. Rev. D 59 (1999) 016004; S.Y. Choi and J.S. Lee, preprint KIAS-P 99066, MADPH-99-1131, September 1999, hep-ph/9907496.

- [18] B. Grzadkowski, J.F. Gunion and J. Kalinowski, preprint UCD-99-1, February 1999, hep-ph/9902308.
- [19] J. Ellis, M.K. Gaillard, D.V. Nanopoulos, Nucl. Phys. B 106 (1976) 292; F. Wilczek, Phys. Rev. Lett. 39 (1977) 1304; H. Georgi, S.L. Glashow, M.E. Machacek and D.V. Nanopoulos, Phys. Rev. Lett. 40 (1978) 692; J. Ellis, M.K. Gaillard, D.V. Nanopoulos and C.T. Sachrajda, Phys. Lett. B 835 (1979) 339; T. Rizzo, Phys. Rev. D 22 (1980) 389; W.-Y. Keung and W.J. Marciano, Phys. Rev. D 30 (1984) 389.
- [20] A. Dedes and S. Moretti, preprint RAL-TR-1999-064, TSL/ISV-99-0211, August 1999, hep-ph/9908516.
- [21] Z. Kunszt and F. Zwimer, Nucl. Phys. B 385 (1992) 3; V. Barger, M. Berger, S. Stange and R. Phillips, Phys. Rev. D 45 (1992) 4128; H. Baer, M. Bisset, C. Kao and X. Tata, Phys. Rev. D 46 (1992) 1067; J.F. Gunion and L. Orr, Phys. Rev. D 46 (1992) 2052; J.F. Gunion, H.E. Haber and C. Kao, Phys. Rev. D 46 (1992) 2907; V. Barger, K. Cheung, R. Phillips and S. Stange, Phys. Rev. D 46 (1992) 4914; H. Baer, M. Bisset, D. Dicus, C. Kao and X. Tata, Phys. Rev. D 47 (1993) 1062.
- [22] A. Kopp, talk given at 'Xth Rencontres de Blois: Frontiers of Matter', Blois, France, June 27-July 3 1999.
- [23] ALEPH Collaboration, contribution to the 'XIX International Symposium on Lepton and Photon Interactions at High Energies', preprint August 1999, hep-ex/9908016.
- [24] D. Stuart, talk given at 'Xth Rencontres de Blois: Frontiers of Matter', Blois, France, June 27-July 3 1999.
- [25] D. Collaboration, preprint Fermilab-Pub-99-046-E, March 1999, hep-ex/9903041.
- [26] D. Collaboration, preprint Fermilab-Pub-98-402-E, February 1999, hep-ex/9902013.
- [27] E. Commins et al., Phys. Rev. A 50 (1994) 2960; K. Abdullah et al., Phys. Rev. Lett. 65 (1990) 2340.
- [28] P.G. Harris et al., Phys. Rev. Lett. 82 (1999) 904.
- [29] S. Dawson, Nucl. Phys. B 359 (1991) 283; S. Dawson and R.P. Kauaman, Phys. Rev. D 49 (1993) 2298; A. Djouadi, M. Spira and P.M. Zerwas, Phys. Lett. B 264 (1991) 440; D. Graudenz, M. Spira and P.M. Zerwas, Phys. Rev. Lett. 70 (1993) 1372; M. Spira, A. Djouadi, D. Graudenz and P.M. Zerwas, Nucl. Phys. B 453 (1995) 17.
- [30] S. Dawson, A. Djouadi and M. Spira, Phys. Rev. Lett. 77 (1996) 16.
- [31] A.D. Martin, R.G. Roberts, W.J. Stirling and R.S. Thorne, Phys. Lett. B 443 (1998) 301.

- [32] A.D. Martin, R.G. Roberts, W.J. Stirling and R.S. Thorne, Eur. Phys. J. C 4 (1998) 463.
- [33] A. Dedes, A.B. Lahanas and K. Tamvakis, Phys. Rev. D 53 (1996) 3793.
- [34] S.M. Barr and A. Zee, Phys. Rev. Lett. 65 (1990) 21.
- [35] D. Chang, W.-Y. Keung and A. Pilaftsis, Phys. Rev. Lett. 82 (1999) 900; Erratum, hep-ph/9811902.
- [36] S. Heinemeyer, W. Hollik and G. Weiglein, Eur. Phys. J. C 9 (1999) 343; S. Heinemeyer, W. Hollik and G. Weiglein, Phys. Lett. B 455 (1999) 179.
- [37] K. Green, private communication.
- [38] J.F. Gunion, H.E. Haber, G.L. Kane and S. Dawson, "The Higgs Hunter's Guide" (Addison-Wesley, Reading MA, 1990) and references therein.
- [39] A. Dedes and S. Moretti, in preparation.

Appendix A : the CP-violating phases in the MSSM

In this Section, we follow the notation of Ref. [38]. We start from the Superpotential, which has the form

$$W = \sum_{ij} Y_e H_1^i L^j E + Y_d H_1^i Q^j D + Y_u H_2^j Q^i U + H_1^i H_2^j \quad (A.1)$$

and where all fields appearing are actually Superfields, with $1, 2 = 1, 2$. In terms of component fields, the Lagrangian of the soft breaking terms reads as

$$\begin{aligned} \mathcal{L}_{\text{soft}} = & -M_{H_1}^2 \tilde{H}_1^2 - M_{H_2}^2 \tilde{H}_2^2 - B_{ij} H_1^i H_2^j + \text{h.c.} \\ & -\frac{1}{2} M_1 \tilde{B} \tilde{B} - \frac{1}{2} M_2 \tilde{W}^a \tilde{W}^a - \frac{1}{2} M_3 \tilde{g} \tilde{g} \\ & -M_Q^2 \tilde{u}_L \tilde{u}_L + \tilde{d}_L \tilde{d}_L - M_U^2 \tilde{u}_R \tilde{u}_R - M_D^2 \tilde{d}_R \tilde{d}_R \\ & -M_L^2 (\tilde{e}_L \tilde{e}_L + \tilde{\nu}_L \tilde{\nu}_L) - M_E^2 \tilde{e}_R \tilde{e}_R \\ & - \sum_{ij} Y_u A_u H_2^i Q^j \tilde{u}_R + Y_d A_d H_1^i Q^j \tilde{d}_R + Y_e A_e H_1^i L^j \tilde{e}_R + \text{h.c.} \quad (A.2) \end{aligned}$$

The squark mass squared matrix (here and in the following, $q^{(0)} = t$ and b)

$$M_q^2 = \begin{pmatrix} M_{qLL}^2 & \mathcal{M}_{qLR}^2 e^{i\varphi} \\ \mathcal{M}_{qRL}^2 e^{i\varphi} & M_{qRR}^2 \end{pmatrix}; \quad (A.3)$$

is Hermitian and can be diagonalised by the unitary transformation

$$U_q^\dagger M_q^2 U_q = \text{diag}(M_{q1}^2, M_{q2}^2); \quad (A.4)$$

with $(M_{q1}^2 < M_{q2}^2)$

$$M_{q(1|2)}^2 = \frac{1}{2} \left[M_{qLL}^2 + M_{qRR}^2 \pm \sqrt{(M_{qLL}^2 - M_{qRR}^2)^2 + 4 |\mathcal{M}_{qRL}^2|^2} \right] \quad (A.5)$$

and

$$U_q = \begin{pmatrix} \cos \varphi_q & \sin \varphi_q e^{i\varphi} \\ \sin \varphi_q e^{i\varphi} & \cos \varphi_q \end{pmatrix}; \quad (A.6)$$

where $\varphi_q = 2\varphi_{q1} - 2\varphi_{q2}$ and

$$\tan 2\varphi_q = \frac{2 |\mathcal{M}_{qRL}^2|}{M_{qLL}^2 - M_{qRR}^2}; \quad (A.7)$$

$$\sin \varphi_q = \frac{|\mathcal{M}_{qRL}^2|}{M_{q(1|2)}^2}; \quad (A.8)$$

where Im refers to the imaginary part of a complex quantity.

Now, in order to construct the Feynman rules for the Higgs-squark-squark vertices, we need the transformation of the squark weak basis $(\tilde{q}_L; \tilde{q}_R)$ into the mass basis $(\tilde{q}_1; \tilde{q}_2)$, namely

$$\begin{pmatrix} \tilde{q}_L \\ \tilde{q}_R \end{pmatrix} = U_q \begin{pmatrix} \tilde{q}_1 \\ \tilde{q}_2 \end{pmatrix} ; \quad (\text{A.9})$$

Furthermore, one has to proceed by also transforming the Higgs boson weak basis $(H_1^0; H_2^0; H_2^+; H_2^-)$ of the four complex fields into the real eight physical ones $(H^0; h^0; A^0; H^+; H^-; G^0; G^+; G^-)$. Following Ref. [38], the transformation can be written as follows

$$H_1^0 = v_1 + \frac{1}{\sqrt{2}} (H^0 \cos \alpha + h^0 \sin \alpha + iA^0 \sin \alpha - iG^0 \cos \alpha) ; \quad (\text{A.10})$$

$$H_2^0 = v_2 + \frac{1}{\sqrt{2}} (H^0 \sin \alpha + h^0 \cos \alpha + iA^0 \cos \alpha + iG^0 \sin \alpha) ; \quad (\text{A.11})$$

$$H_1^+ = H^+ \sin \beta + G^+ \cos \beta ; \quad (\text{A.12})$$

$$H_2^+ = H^+ \cos \beta + G^+ \sin \beta ; \quad (\text{A.13})$$

with $(H^\pm) = H$ and

$$\sin 2\beta = \frac{\sin 2\alpha}{\frac{M_{H^0}^2 + M_{h^0}^2}{M_{H^0}^2 - M_{h^0}^2}} ; \quad (\text{A.14})$$

where $M_{H^0}; M_{h^0}$ are the tree-level CP-even Higgs boson masses.

The Feynman rules for the Higgs-squark-squark vertices, involving mixing and phases, namely are (here, $\alpha = 0$ and $H = 0$):

$$\begin{aligned} \tilde{q}_1 \tilde{q}_1^0 &= C_q C_q^0 \tilde{q}_L \tilde{q}_L^0 + S_q S_q^0 \tilde{q}_R \tilde{q}_R^0 + C_q S_q^0 e^{i\alpha^0} \tilde{q}_L \tilde{q}_R^0 + S_q C_q^0 e^{-i\alpha} \tilde{q}_R \tilde{q}_L^0 ; \\ \tilde{q}_2 \tilde{q}_2^0 &= S_q S_q^0 \tilde{q}_L \tilde{q}_L^0 + C_q C_q^0 \tilde{q}_R \tilde{q}_R^0 - S_q C_q^0 e^{i\alpha} \tilde{q}_L \tilde{q}_R^0 - C_q S_q^0 e^{-i\alpha^0} \tilde{q}_R \tilde{q}_L^0 ; \\ \tilde{q}_1 \tilde{q}_2^0 &= C_q S_q^0 e^{-i\alpha^0} \tilde{q}_L \tilde{q}_L^0 + S_q C_q^0 e^{-i\alpha} \tilde{q}_R \tilde{q}_R^0 + C_q C_q^0 \tilde{q}_L \tilde{q}_R^0 - S_q S_q^0 e^{i(\alpha^+ - \alpha^0)} \tilde{q}_R \tilde{q}_L^0 ; \\ \tilde{q}_2 \tilde{q}_1^0 &= S_q C_q^0 e^{i\alpha} \tilde{q}_L \tilde{q}_L^0 + C_q S_q^0 e^{i\alpha^0} \tilde{q}_R \tilde{q}_R^0 - S_q S_q^0 e^{i(\alpha^0 + \alpha)} \tilde{q}_L \tilde{q}_R^0 + C_q C_q^0 \tilde{q}_R \tilde{q}_L^0 ; \end{aligned} \quad (\text{A.15})$$

For the case of stop squarks (i.e., $q = t$), one has

$$M_{\tilde{t}L}^2 = M_Q^2 + M_t^2 + \frac{1}{6} (4M_W^2 - M_Z^2) \cos 2\beta ; \quad (\text{A.16})$$

$$M_{\tilde{t}R}^2 = M_U^2 + M_t^2 - \frac{2}{3} (M_W^2 - M_Z^2) \cos 2\beta ; \quad (\text{A.17})$$

$$M_{\tilde{t}RL}^2 = (M_{\tilde{t}LR}^2) = m_t (A_t + \cot \beta) ; \quad (\text{A.18})$$

and thus

$$\tan 2\tau = \frac{2m_t \tilde{A}_t + \cot \beta}{M_Q^2 - M_U^2 + \frac{4}{3}M_W^2 - \frac{5}{6}M_Z^2 \cos 2\beta}; \quad (\text{A } 19)$$

$$\sin \tau = \frac{\tilde{A}_t j \sin A_t - j j \sin \cot}{\tilde{A}_t + \cot \beta}; \quad (\text{A } 20)$$

where $\beta = \beta - \beta^i$ and $A_t = \tilde{A}_t \beta^i A_t$.

Similarly, one obtains for sbottoms (i.e., $q = b$):

$$M_{BL}^2 = M_Q^2 + m_b^2 - \frac{1}{6}(2M_W^2 + M_Z^2) \cos 2\beta; \quad (\text{A } 21)$$

$$M_{BR}^2 = M_D^2 + m_b^2 + \frac{1}{3}(M_W^2 - M_Z^2) \cos 2\beta; \quad (\text{A } 22)$$

$$M_{BR}^2 - M_{BL}^2 = m_b(A_b + \tan \beta); \quad (\text{A } 23)$$

with

$$\tan 2\beta = \frac{2m_b \tilde{A}_b + \tan \beta}{M_Q^2 - M_D^2 + \frac{2}{3}M_W^2 + \frac{1}{6}M_Z^2 \cos 2\beta}; \quad (\text{A } 24)$$

$$\sin \beta = \frac{\tilde{A}_b j \sin A_b - j j \sin \tan}{\tilde{A}_b + \tan \beta}; \quad (\text{A } 25)$$

where $A_b = \tilde{A}_b \beta^i A_b$.

The chiral couplings $\kappa_{q\bar{q}^0}^0$ ($q = L, R$) of eq. (A 15) can be found in Ref. [38], with the only exception of those cases where β and A_q enter³, for which one has to adopt the following set of formulae (with $g^2 = 4e_{EM}^2 = \sin^2 \theta_W$ the weak constant and where M_W is the W boson mass):

$$A^0 \bar{t}_L t_R = \frac{gm_u}{2M_W} (A_u \cot \beta); \quad (\text{A } 26)$$

$$A^0 \bar{t}_L t_R = (A^0 \bar{t}_L t_R); \quad (\text{A } 27)$$

$$A^0 \bar{b}_L b_R = \frac{gm_d}{2M_W} (A_d \tan \beta); \quad (\text{A } 28)$$

$$A^0 \bar{b}_L b_R = (A^0 \bar{b}_L b_R); \quad (\text{A } 29)$$

$$H^0 \bar{t}_L t_R = \frac{igm_u}{2M_W \sin \beta} (\cos \beta + A_u \sin \beta); \quad (\text{A } 30)$$

$$H^0 \bar{t}_L t_R = (H^0 \bar{t}_L t_R); \quad (\text{A } 31)$$

$$H^0 \bar{b}_L b_R = \frac{igm_d}{2M_W \cos \beta} (\sin \beta + A_d \cos \beta); \quad (\text{A } 32)$$

³In other terms, for real β and A_q our expressions reduce to those in Ref. [38].

$$H^0 \tilde{b}_L \tilde{b}_R = (H^0 \tilde{b}_L \tilde{b}_R) ; \quad (A.33)$$

$$h^0 \tilde{t}_L \tilde{t}_R = \frac{igm_u}{2M_W \sin} (\sin A_u \cos) ; \quad (A.34)$$

$$h^0 \tilde{t}_L \tilde{t}_R = (h^0 \tilde{t}_L \tilde{t}_R) ; \quad (A.35)$$

$$h^0 \tilde{b}_L \tilde{b}_R = \frac{igm_d}{2M_W \cos} (\cos A_d \sin) ; \quad (A.36)$$

$$h^0 \tilde{b}_L \tilde{b}_R = (h^0 \tilde{b}_L \tilde{b}_R) ; \quad (A.37)$$

$$H^+ \tilde{b}_L \tilde{t}_R = \frac{igm_u}{2M_W} (A_u \cot) ; \quad (A.38)$$

$$H^- \tilde{t}_L \tilde{b}_R = \frac{igm_d}{2M_W} (A_d \tan) ; \quad (A.39)$$

$$H^+ \tilde{t}_L \tilde{b}_R = \frac{igm_d}{2M_W} (A_d \tan) ; \quad (A.40)$$

$$H^- \tilde{b}_L \tilde{t}_R = \frac{igm_u}{2M_W} (A_u \cot) ; \quad (A.41)$$

(Although we have not made use of the Feynman rules involving charged Higgses we display them here for completeness.) We need also the interactions among Higgs bosons and quarks and these read as follows:

$$A^0 tt = \frac{gm_u \cot}{2M_W} ; \quad (A.42)$$

$$A^0 bb = \frac{gm_d \tan}{2M_W} ; \quad (A.43)$$

$$H^0 tt = \frac{igm_u \sin}{2M_W \sin} ; \quad (A.44)$$

$$H^0 bb = \frac{igm_d \cos}{2M_W \cos} ; \quad (A.45)$$

$$h^0 tt = \frac{igm_u \cos}{2M_W \sin} ; \quad (A.46)$$

$$h^0 bb = \frac{igm_d \sin}{2M_W \cos} ; \quad (A.47)$$

It is now useful to look at the explicit phase dependence of the vertices involving Higgs bosons and squarks: to this end, we expand our formulae (A.15). The relevant couplings

involving the CP-odd Higgs boson read as⁴:

$$\begin{aligned}
A^0 t_1 t_1 &= i \frac{g m_t}{2 M_W} \sin 2 \tau \left[j \sin(\tau) \right] - A_t j \sin(\tau + A_t) \cot \tau ; \\
A^0 t_2 t_2 &= A^0 t_1 t_1 ; \\
A^0 b_1 b_1 &= i \frac{g m_b}{2 M_W} \sin 2 \beta \left[j \sin(\beta) \right] - A_b j \sin(\beta + A_b) \tan \beta ; \\
A^0 b_2 b_2 &= A^0 b_1 b_1 ;
\end{aligned} \tag{A.48}$$

For the CP-even Higgs bosons we find (here, $s_W = \sin \theta_W$),

$$\begin{aligned}
H^0 t_1 t_1 &= \frac{i g M_Z}{C_W} \left[\frac{h_1}{2} \cos^2 \tau - e_d s_W^2 \cos 2 \tau \cos(\tau + A_t) \right] \frac{m_t^2}{M_Z^2} \frac{\sin \tau}{\sin \tau} \\
&\quad + \frac{m_t \sin 2 \tau}{2 M_Z^2 \sin \tau} \left[j \cos(\tau) \cos \tau + A_t j \cos(\tau + A_t) \sin \tau \right] ; \tag{A.49}
\end{aligned}$$

$$\begin{aligned}
H^0 t_2 t_2 &= \frac{i g M_Z}{C_W} \left[\frac{h_1}{2} \sin^2 \tau + e_u s_W^2 \cos 2 \tau \cos(\tau + A_t) \right] \frac{m_t^2}{M_Z^2} \frac{\sin \tau}{\sin \tau} \\
&\quad + \frac{m_t \sin 2 \tau}{2 M_Z^2 \sin \tau} \left[j \cos(\tau) \cos \tau + A_t j \cos(\tau + A_t) \sin \tau \right] ; \tag{A.50}
\end{aligned}$$

$$\begin{aligned}
H^0 b_1 b_1 &= \frac{i g M_Z}{C_W} \left[\frac{h_1}{2} \cos^2 \beta + e_d s_W^2 \cos 2 \beta \cos(\beta + A_b) \right] \frac{m_b^2}{M_Z^2} \frac{\cos \beta}{\cos \beta} \\
&\quad + \frac{m_b \sin 2 \beta}{2 M_Z^2 \cos \beta} \left[j \cos(\beta) \sin \beta + A_b j \cos(\beta + A_b) \cos \beta \right] ; \tag{A.51}
\end{aligned}$$

$$\begin{aligned}
H^0 b_2 b_2 &= \frac{i g M_Z}{C_W} \left[\frac{h_1}{2} \sin^2 \beta - e_u s_W^2 \cos 2 \beta \cos(\beta + A_b) \right] \frac{m_b^2}{M_Z^2} \frac{\cos \beta}{\cos \beta} \\
&\quad + \frac{m_b \sin 2 \beta}{2 M_Z^2 \cos \beta} \left[j \cos(\beta) \sin \beta + A_b j \cos(\beta + A_b) \cos \beta \right] ; \tag{A.52}
\end{aligned}$$

$$\begin{aligned}
h^0 t_1 t_1 &= \frac{i g M_Z}{C_W} \left[\frac{h_1}{2} \cos^2 \tau - e_d s_W^2 \cos 2 \tau \sin(\tau + A_t) \right] \frac{m_t^2}{M_Z^2} \frac{\cos \tau}{\sin \tau} \\
&\quad + \frac{m_t \sin 2 \tau}{2 M_Z^2 \sin \tau} \left[j \cos(\tau) \sin \tau - A_t j \cos(\tau + A_t) \cos \tau \right] ; \tag{A.53}
\end{aligned}$$

$$h^0 t_2 t_2 = \frac{i g M_Z}{C_W} \left[\frac{h_1}{2} \sin^2 \tau + e_u s_W^2 \cos 2 \tau \sin(\tau + A_t) \right] \frac{m_t^2}{M_Z^2} \frac{\cos \tau}{\sin \tau}$$

⁴Note that the vertices with gluons and squarks are not affected by the phases.

$$\frac{m_t \sin 2\beta}{2M_Z^2 \sin\beta} \frac{h}{j} j \cos(\beta - \alpha_t) \sin \alpha_t \tilde{A}_t j \cos(\beta - \alpha_t) \cos \alpha_t^i; \quad (\text{A.54})$$

$$h^0 B_1 B_1 = \frac{igM_Z}{C_W} \frac{n}{2} \frac{h}{j} \cos^2 \beta + e_d s_W^2 \cos 2\beta \sin(\beta + \alpha_b) + \frac{m_b^2 \sin\beta}{M_Z^2 \cos\beta} \frac{h}{j} j \cos(\beta - \alpha_b) \cos \alpha_b \tilde{A}_b j \cos(\beta - \alpha_b) \sin \alpha_b^i; \quad (\text{A.55})$$

$$h^0 B_2 B_2 = \frac{igM_Z}{C_W} \frac{n}{2} \frac{h}{j} \sin^2 \beta - e_u s_W^2 \cos 2\beta \sin(\beta + \alpha_t) + \frac{m_b^2 \sin\beta}{M_Z^2 \cos\beta} \frac{h}{j} j \cos(\beta - \alpha_b) \cos \alpha_b \tilde{A}_b j \cos(\beta - \alpha_b) \sin \alpha_b^i; \quad (\text{A.56})$$

where $e_u = +2/3$ and $e_d = -1/3$. Of course, one can get the corresponding vertices for all squarks flavours by a simple substitution $t \rightarrow u; c$ and $b \rightarrow d; s$.

Appendix B : matrix elements and cross sections

Since, as we have already discussed in the main body of the paper, the CP-violating phases induce a non-zero contribution from squark loops in CP-odd Higgs boson production which is absent in the phaseless MSSM and since this has not been evaluated yet in the literature, we had to perform the loop tensor reduction in such a case from scratch. However, for comparison purposes, we have also recalculated the well known tensor associated to CP-even Higgs boson production and found agreement with old results. We have evaluated the diagrams in the (modified) Dimensional Regularisation (DR) scheme, which preserves the SUSY Ward identities of the theory up to two loops. This enabled us to check analytically the gauge invariance of our results. Furthermore, we have carried out the ϵ -algebra in four dimensions while using analytical continuation in d dimensions in order to calculate the divergent parts of the integrals. The squared matrix elements summed/averaged over final/initial spins and colours⁵ are:

$$\begin{aligned} \overline{M}_{gg \rightarrow h^0}^2 &= \frac{2}{256} \frac{(Q)M_{h^0}^4}{s^2} \sum_q \frac{h^0_{qq}}{m_q} \frac{h}{j} j 1 + (1 - \cos^2 \beta) f(\beta) \frac{1}{4} \sum_q \frac{h^0_{qq}}{m_q^2} \frac{h}{j} j 1 - \cos^2 \beta f(\beta)^2; \\ \overline{M}_{gg \rightarrow H^0}^2 &= \frac{2}{256} \frac{(Q)M_{H^0}^4}{s^2} \sum_q \frac{H^0_{qq}}{m_q} \frac{h}{j} j 1 + (1 - \cos^2 \beta) f(\beta) \frac{1}{4} \sum_q \frac{H^0_{qq}}{m_q^2} \frac{h}{j} j 1 - \cos^2 \beta f(\beta)^2; \\ \overline{M}_{gg \rightarrow A^0}^2 &= \frac{2}{256} \frac{(Q)M_{A^0}^4}{s^2} \sum_q \frac{A^0_{qq}}{m_q} \frac{h}{j} j f(\beta)^2 + \frac{1}{16} \sum_q \frac{A^0_{qq}}{m_q^2} \frac{h}{j} j 1 - \cos^2 \beta f(\beta)^2 \quad (\text{B.1}) \end{aligned}$$

⁵Note that the ϵ -matrix is here intended to be removed from the expressions of the A^0_{qq} 's of eqs. (A.43)-(A.44).

where $q_{\text{eff}} = \frac{4m_q^2}{M_{\tilde{g}}^2}$, $q = t, b$ and $\bar{q} = \bar{t}_1, \bar{t}_2, \bar{b}_1, \bar{b}_2$. The function $f(\cdot)$ stands for

$$f(\cdot) = \frac{1}{2} \int_0^1 \frac{dy}{y} \ln \left(1 + \frac{4y(1-y)}{q_{\text{eff}}} \right) = \begin{cases} \arcsin^2(\sqrt{q_{\text{eff}}}); & q_{\text{eff}} \geq 1; \\ \frac{1}{4} \ln \frac{1+\sqrt{1-q_{\text{eff}}}}{1-\sqrt{1-q_{\text{eff}}}} - \frac{i}{2}; & q_{\text{eff}} < 1; \end{cases} \quad (\text{B.2})$$

and some useful limits are

$$\lim_{q_{\text{eff}} \rightarrow 1} \left(1 + (1 - q_{\text{eff}}) f(\cdot) \right) = +\frac{2}{3}; \quad (\text{B.3})$$

$$\lim_{q_{\text{eff}} \rightarrow 1} \left(1 - q_{\text{eff}} f(\cdot) \right) = \frac{1}{3}; \quad (\text{B.4})$$

$$\lim_{q_{\text{eff}} \rightarrow 0} f(\cdot) = +1; \quad (\text{B.5})$$

The non-existence of interference terms between quark and squark loops for CP-odd Higgs boson production can readily be understood by looking at the corresponding amplitude formula (P_1, P_2 are the gluon four-momenta, $(P_1), (P_2)$ their polarisation four-vectors and a, b their colours)

$$i(P_1)(P_2)M_{ab}(gg \rightarrow A^0) = \frac{s(Q)}{2} \epsilon_{ab}(P_1)(P_2) \\ + i \epsilon_{ab} P_1 P_2 \sum_q \frac{A^0 q q}{m_q} \left(1 + (1 - q_{\text{eff}}) f(q_{\text{eff}}) \right) + \frac{1}{4} \sum_q \frac{A^0 q q}{m_q^2} g(P_1) g(P_2) P_1 P_2 \left(1 - q_{\text{eff}} f(q_{\text{eff}}) \right); \quad (\text{B.6})$$

where one notices an antisymmetric part (note the Levi-Civita tensor ϵ associated to the quark contributions (first term on the right-hand side) and a symmetric one associated to the squark loops (second term on the right-hand side). For completeness, we also give the tensor structure of the loop amplitudes corresponding to CP-even Higgs boson production:

$$i(P_1)(P_2)M_{ab}(gg \rightarrow h^0; H^0) = \frac{s(Q)}{2} \epsilon_{ab}(P_1)(P_2) g(P_1) g(P_2) P_1 P_2 \\ + \sum_q \frac{(h^0; H^0) q q}{m_q} \left(1 + (1 - q_{\text{eff}}) f(q_{\text{eff}}) \right) + \frac{1}{4} \sum_q \frac{(h^0; H^0) q q}{m_q^2} g(P_1) g(P_2) P_1 P_2 \left(1 - q_{\text{eff}} f(q_{\text{eff}}) \right); \quad (\text{B.7})$$

Here, interference effects clearly exist between the SM- and SUSY-like parts, because of the symmetric nature of both contributions.

The LO partonic cross sections at the energy $\sqrt{\hat{s}}$ are then

$$\hat{\sigma}_{\text{LO}}^0 = \frac{1}{\hat{s}} \overline{M}_{gg \rightarrow A^0}^2(\hat{s} = M_{A^0}^2); \quad (\text{B.8})$$

whereas the corresponding hadronic rates for a collider CM energy \sqrt{s} read as

$$\sigma_{LO}^0 = \frac{1}{M_0^4} \overline{M}^2 f_{gg}^2 \frac{dL}{d} ; \quad (B.9)$$

with $\frac{dL}{d} = \frac{s}{M_0^2}$ and

$$\frac{dL}{d} = \int_0^1 \frac{dx}{x} g(x; Q) g\left(\frac{1}{x}; Q\right) ; \quad (B.10)$$

where $g(x; Q)$ is the PDF of the gluon, evaluated at the scale $Q = M_0$.

As already mentioned in the Introduction, in performing the two-loop analysis, we have made use of the formulae given in Ref. [30]. We refer the reader to that paper for specific details.

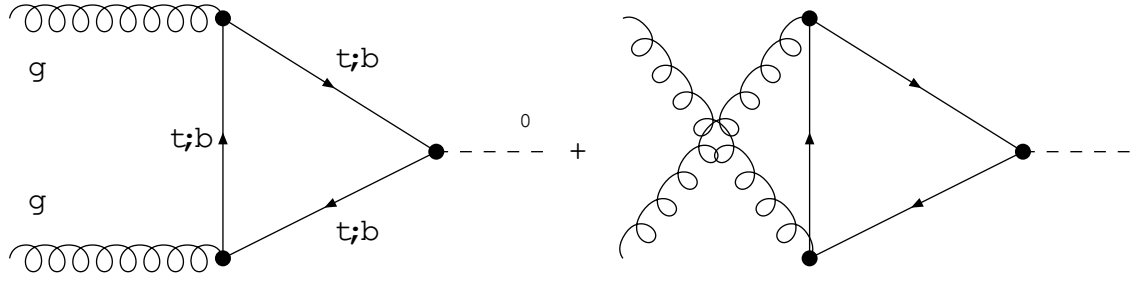


Figure 1: SM-like contributions from top (t) and bottom (b) quarks to Higgs boson production via $gg \rightarrow H^0$ in the MSSM.

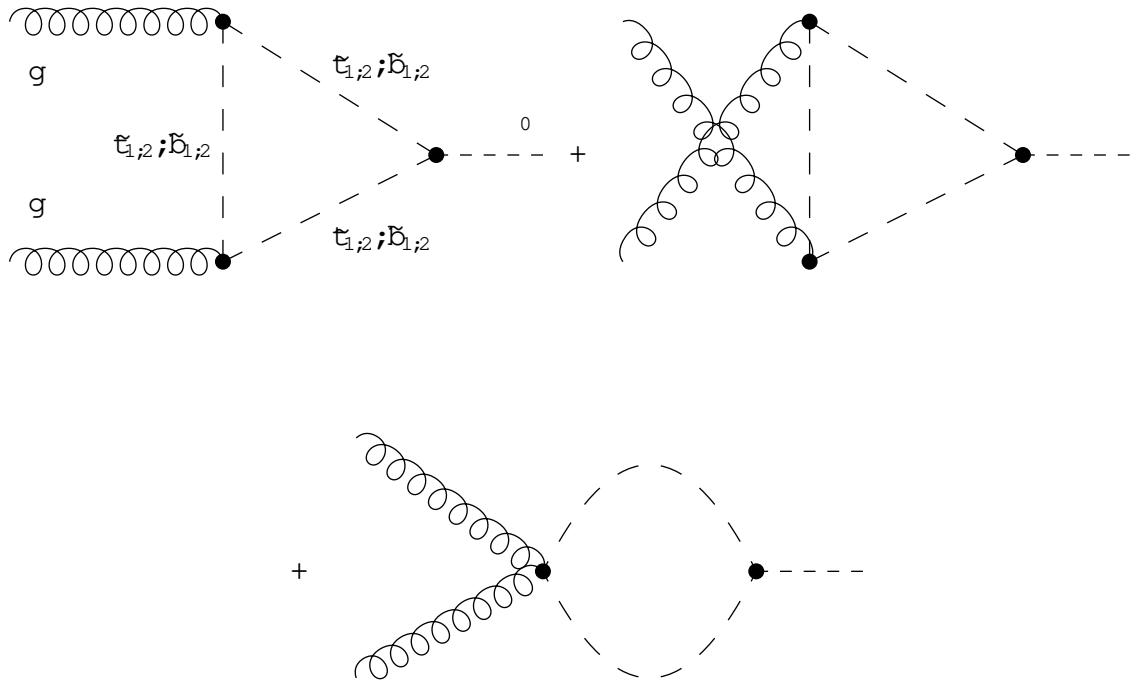


Figure 2: SUSY-like contributions from top ($\tilde{t}_{1,2}$) and bottom ($\tilde{b}_{1,2}$) squarks to Higgs boson production via $gg \rightarrow H^0$ in the MSSM. (Notice that, if the CP-symmetry is conserved, then $H^0 \notin A^0$.)

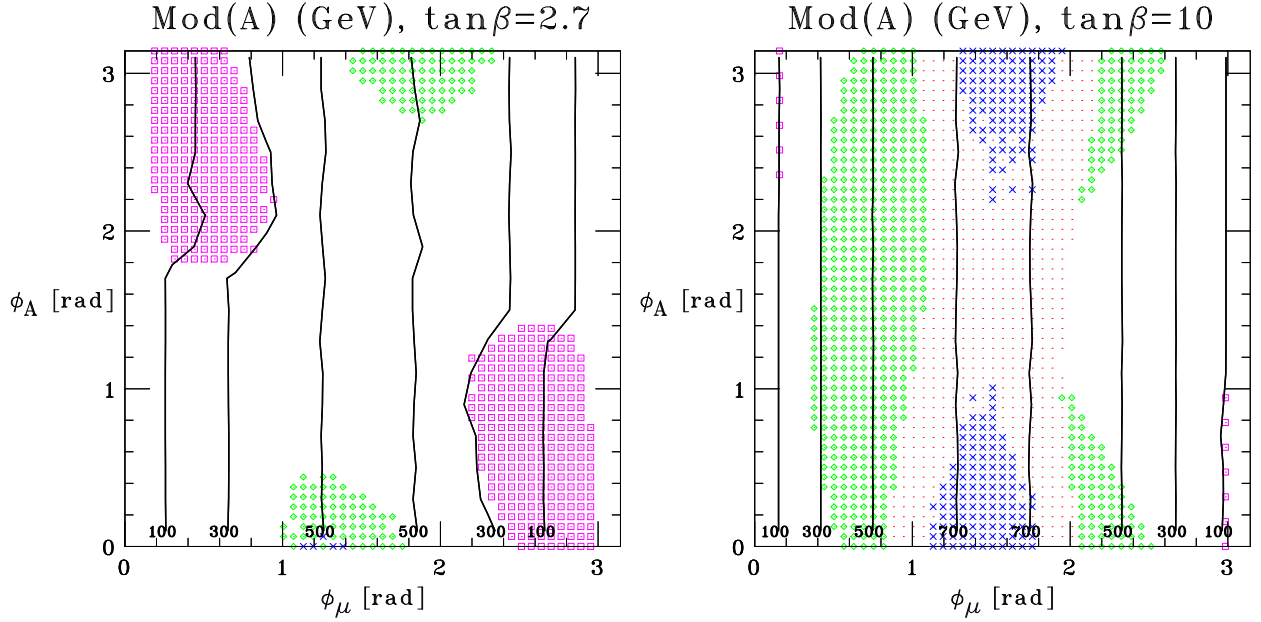


Figure 3: Contour plots for the values of the modulus of the common trilinear coupling, $|A_j|$, needed in order to obtain the cancellations of the SUSY contributions to the one-loop EDMs, over the $(\phi_\mu; \phi_A)$ plane for small (left-hand plot) and large (right-hand plot) $\tan\beta$. The other MSSM parameters are as given in Tab. I. Here and in the following, \times symbols denote points excluded because of the negativity of the squark masses squared; \square symbols denote points excluded by the two-loop Zee-Barr type contributions to the EDMs; \circ and \triangle symbols denote points excluded from Higgs boson and squark direct searches, respectively.

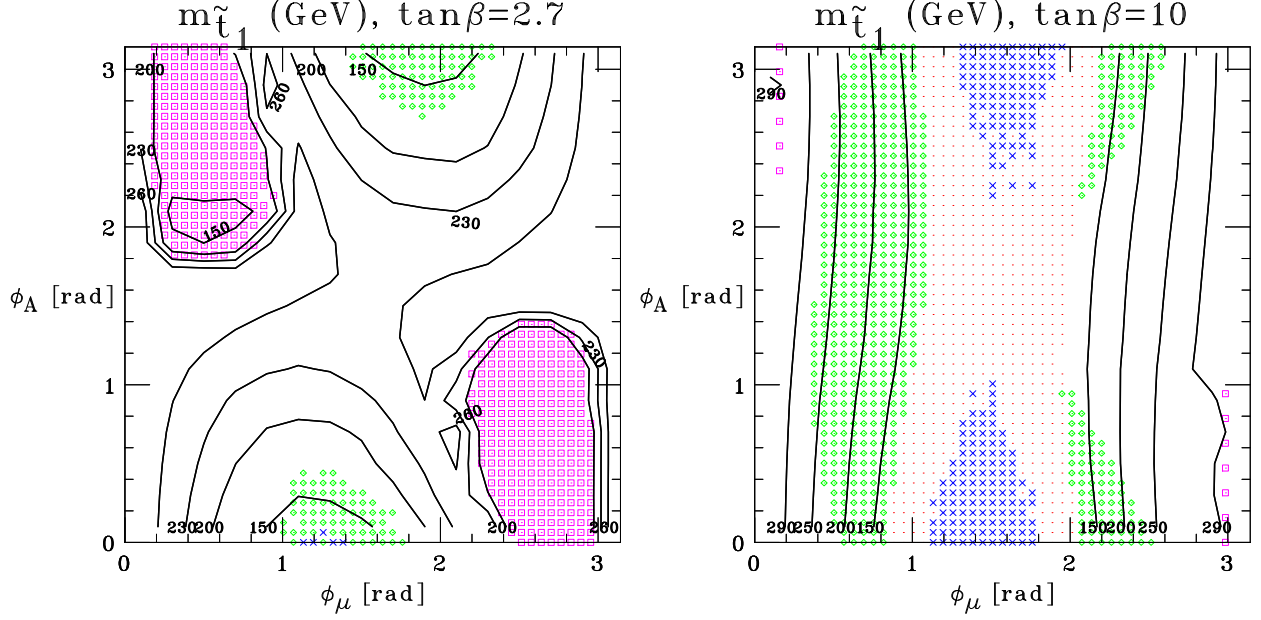


Figure 4: Contour plots for the values of the lightest top squark mass, $m_{\tilde{t}_1}$, corresponding to those of $\tilde{A}j$ in Fig. 3, over the $(\phi_\mu; \phi_A)$ plane for small (left-hand plot) and large (right-hand plot) $\tan\beta$. The other MSSM parameters are as given in Tab. I.

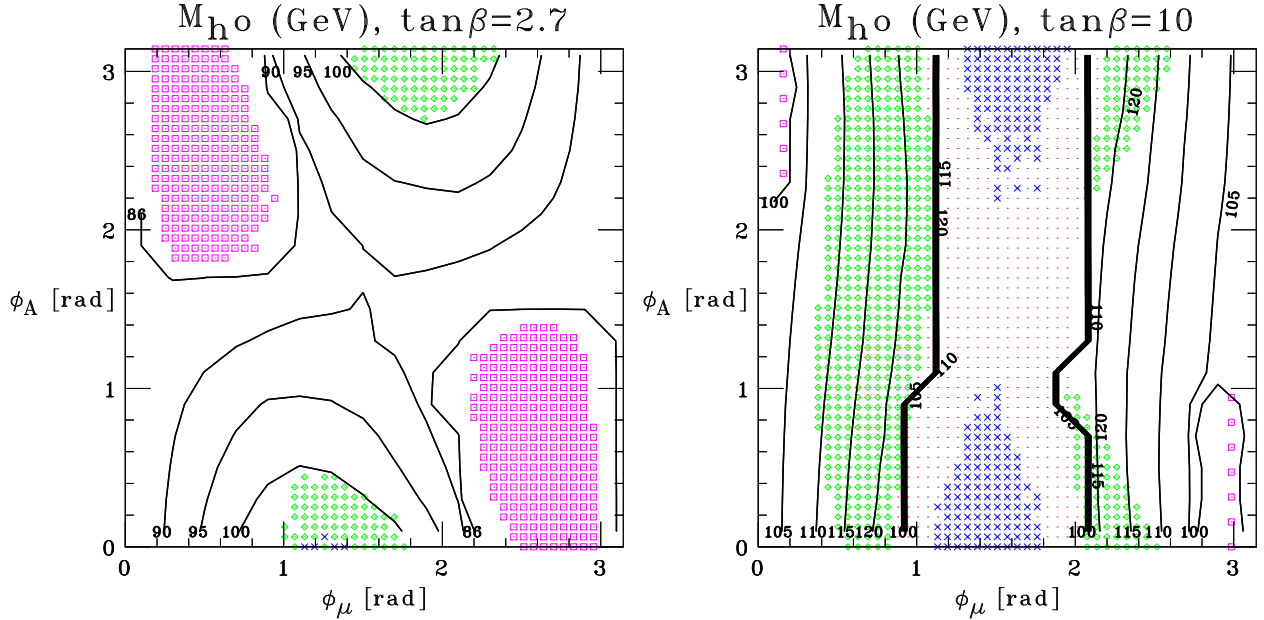


Figure 5: Contour plots for the values of the lightest Higgs boson mass, M_{h^0} , corresponding to those of $\tilde{A}j$ in Fig. 3, over the $(\phi_\mu; \phi_A)$ plane for small (left-hand plot) and large (right-hand plot) $\tan\beta$. The other MSSM parameters are as given in Tab. I.

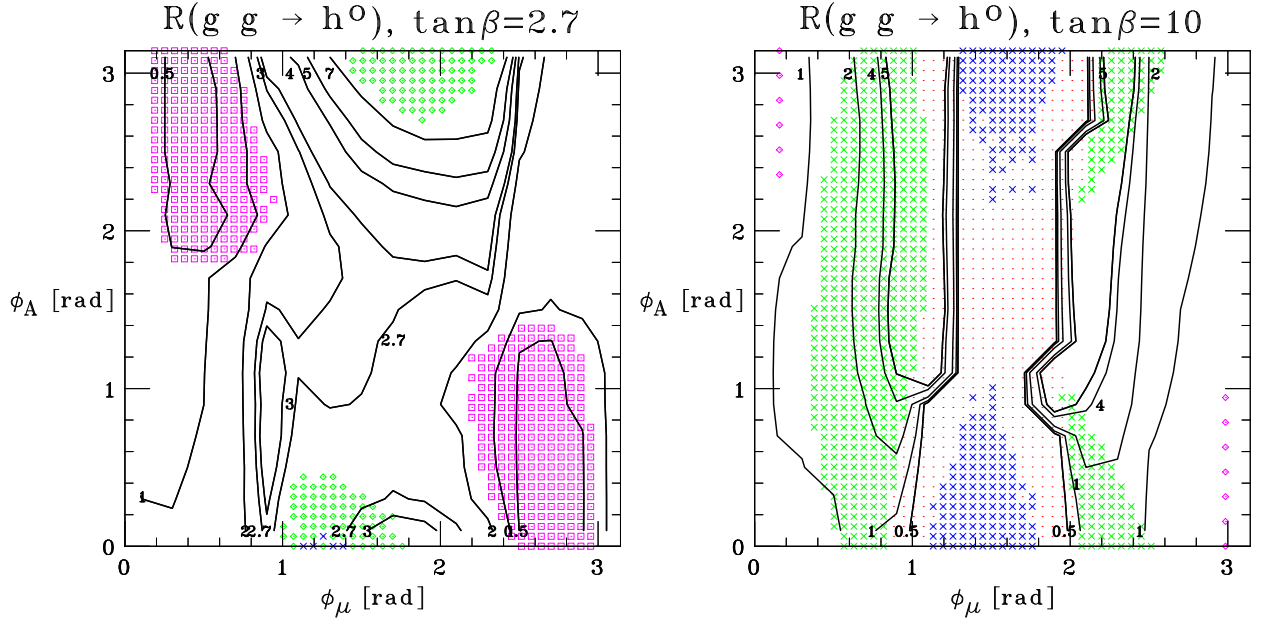


Figure 6: Contour plots for the values of the ratio in eq. (7) for the case $h^0 = h^0$, corresponding to those of $\tilde{A}j$ in Fig. 3, over the $(\phi_\mu; \phi_A)$ plane for small (left-hand plot) and large (right-hand plot) $\tan\beta$. The other MSSM parameters are as given in Tab. I.

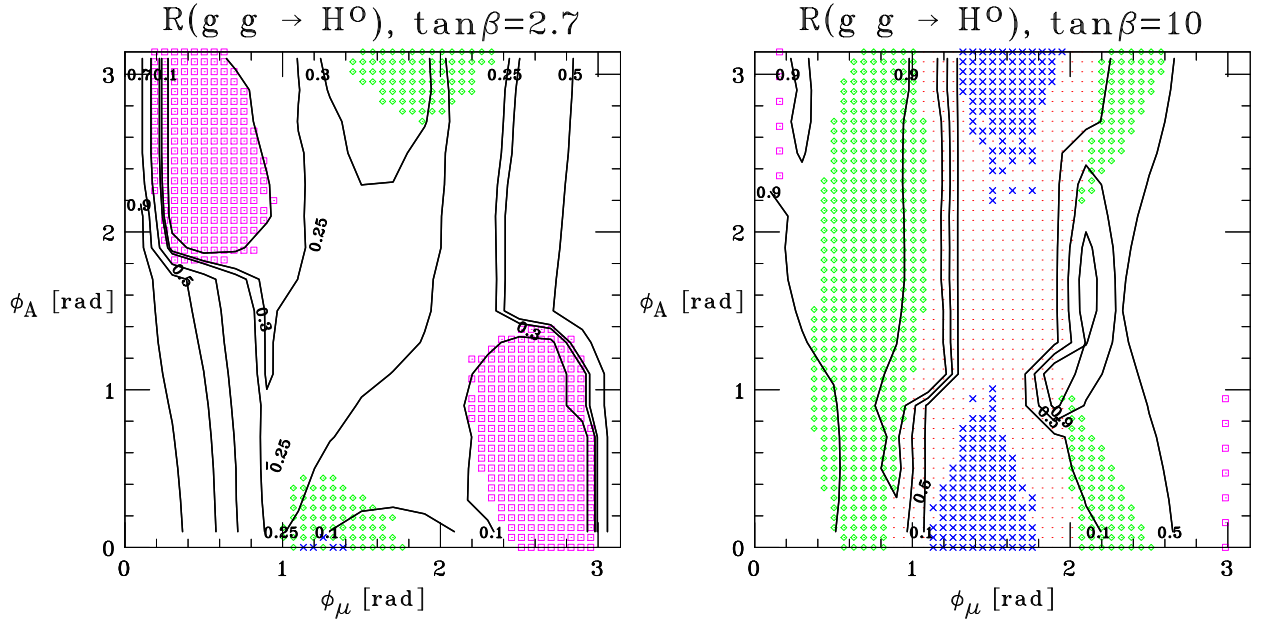


Figure 7: Same as in Fig. 6 for the case $h^0 = H^0$.

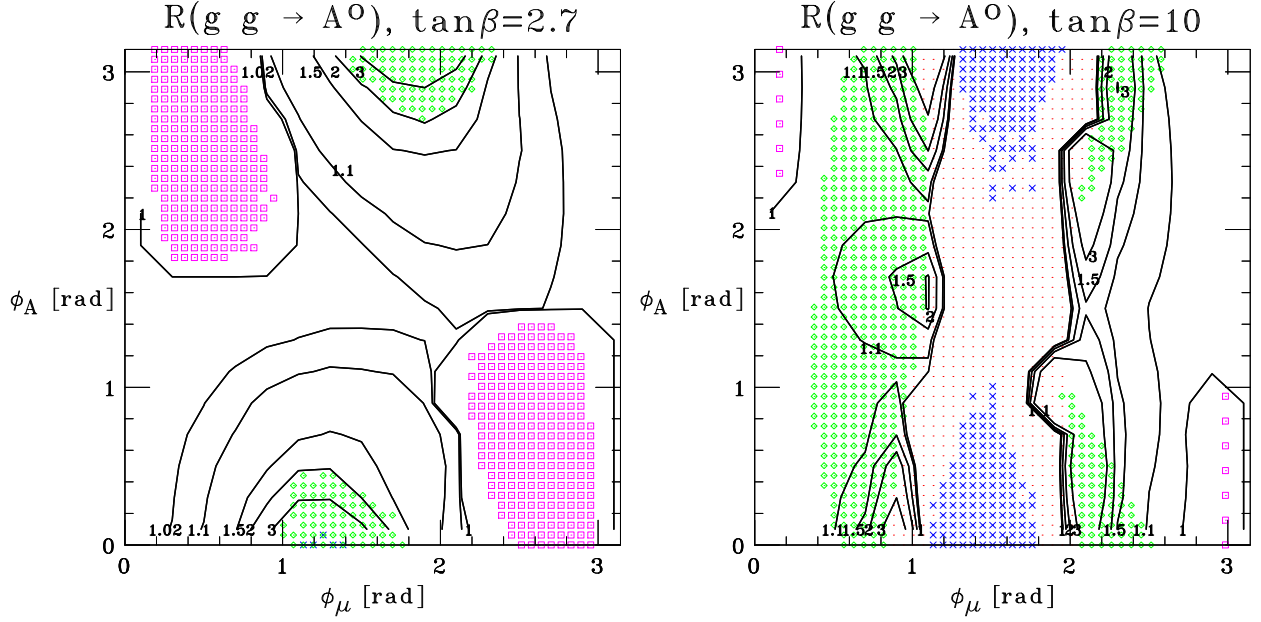


Figure 8: Same as in Fig. 6 for the case $\phi_0 = A^0$.

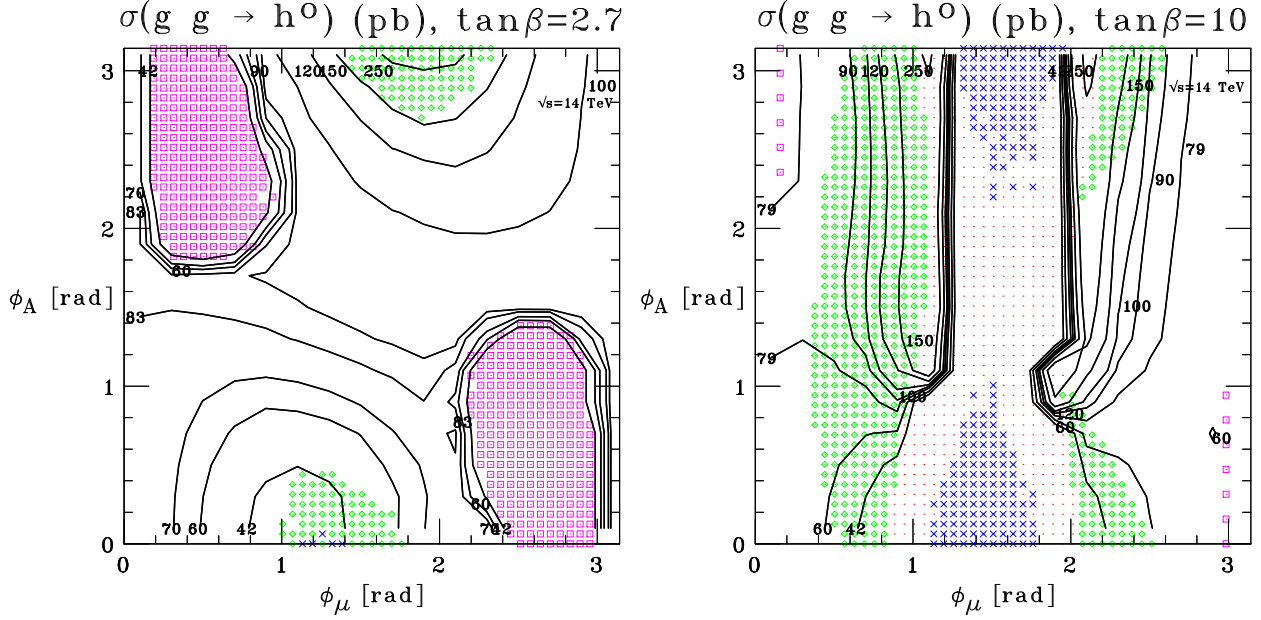


Figure 9: Contour plots for the values of the NLO cross section for $gg \rightarrow h^0$ in the MSSM at the LHC, $\sigma_{\text{NLO}}^{\text{MSSM}}(gg \rightarrow h^0)$, for the case $\phi_0 = h^0$, corresponding to those of \mathcal{A}_j in Fig. 3, over the $(\phi_\mu; \phi_A)$ plane for small (left-hand plot) and large (right-hand plot) $\tan\beta$. The other MSSM parameters are as given in Tab. I.

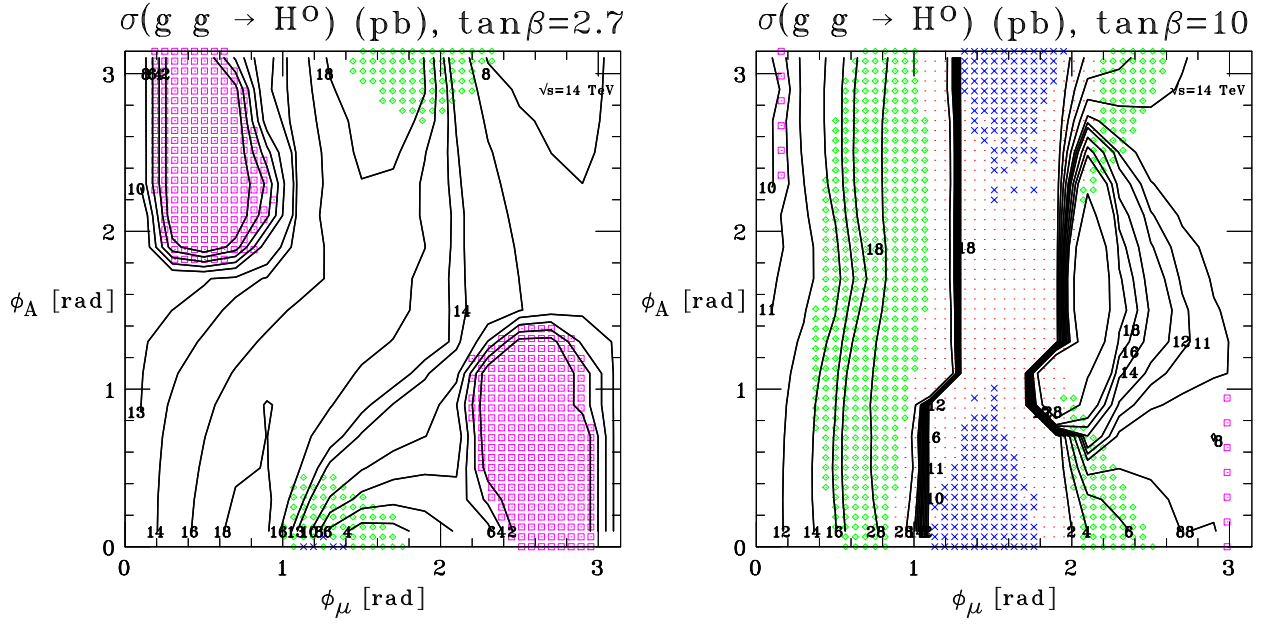


Figure 10: Same as in Fig. 9 for the case $^0 = H^0$.

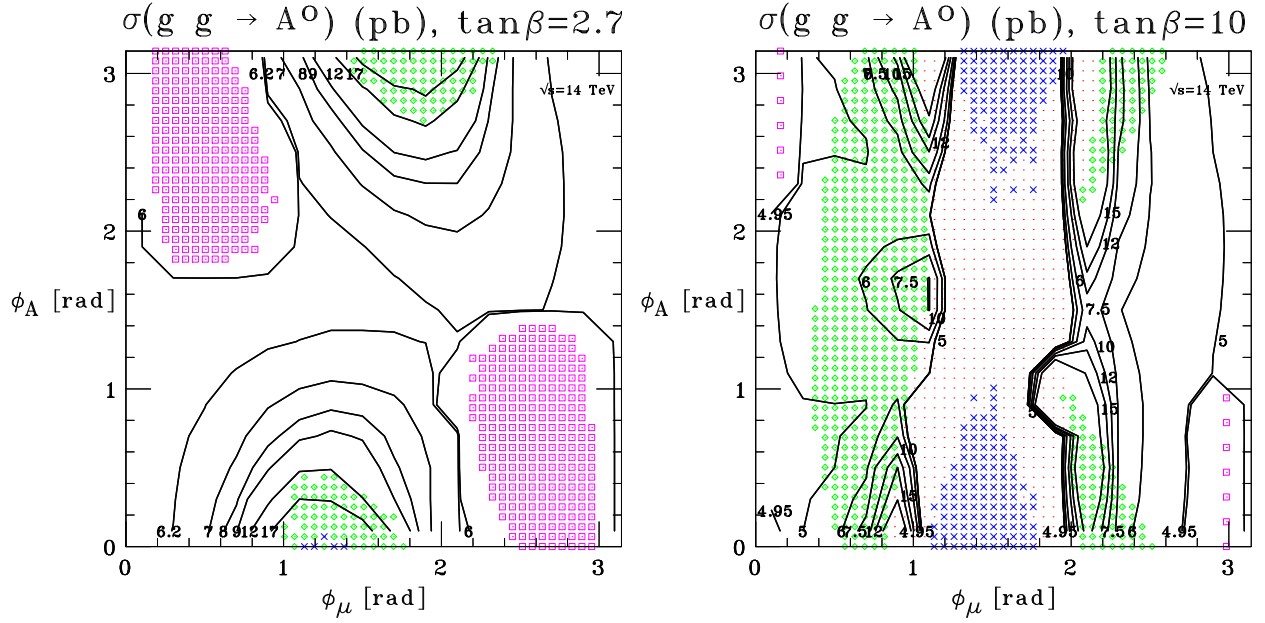


Figure 11: Same as in Fig. 9 for the case $^0 = A^0$.

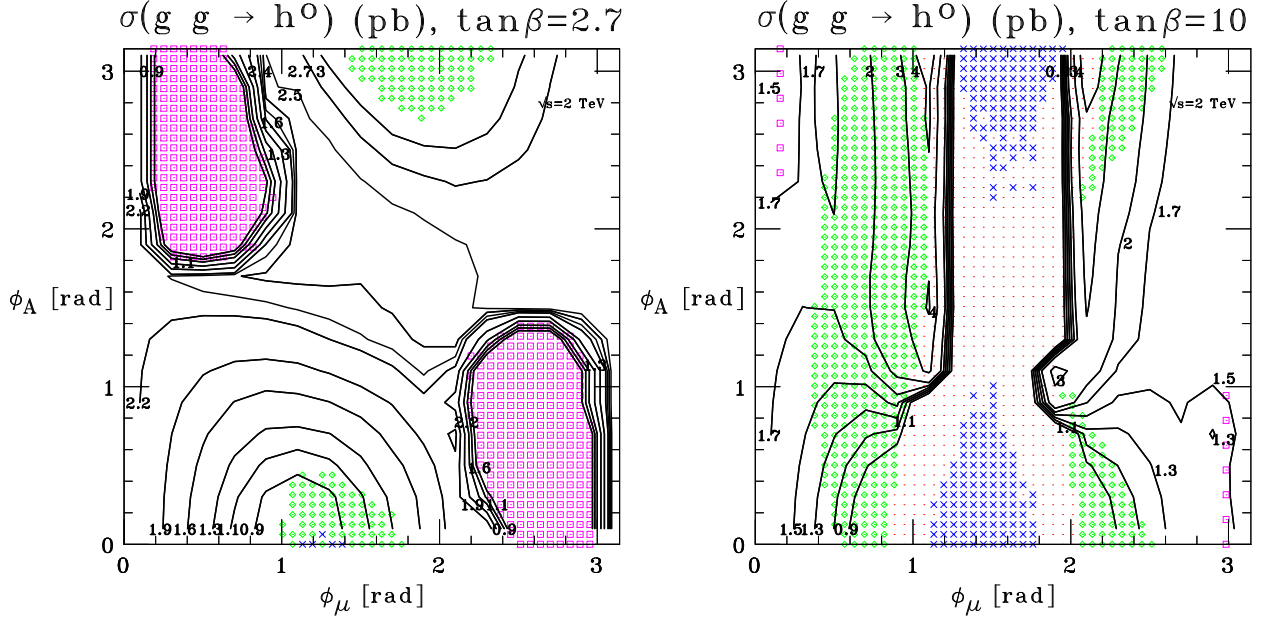


Figure 12: Contour plots for the values of the NLO cross section for $gg \rightarrow h^0$ in the MSSM at the Tevatron, $\sigma_{\text{NLO}}^{\text{MSSM}}(gg \rightarrow h^0)$, for the case $h^0 = h^0$, corresponding to those of \mathcal{A}_j in Fig. 3, over the $(\phi_\mu; \phi_A)$ plane for small (left-hand plot) and large (right-hand plot) $\tan \beta$. The other MSSM parameters are as given in Tab. I.

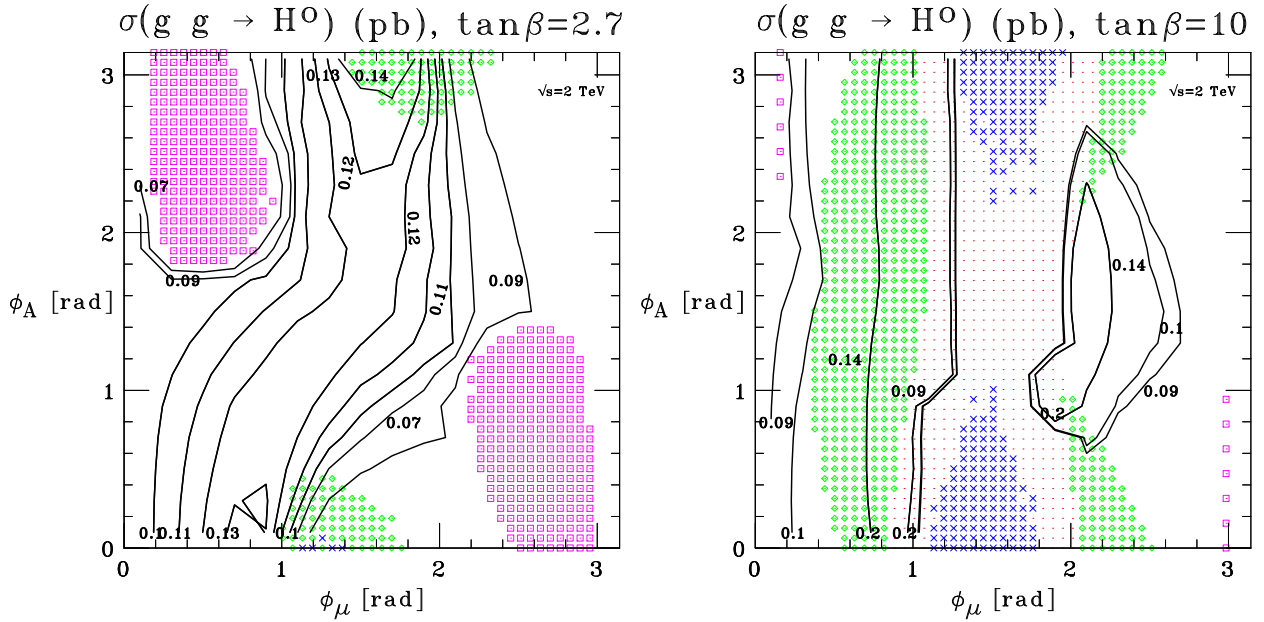


Figure 13: Same as in Fig. 12 for the case $h^0 = H^0$.

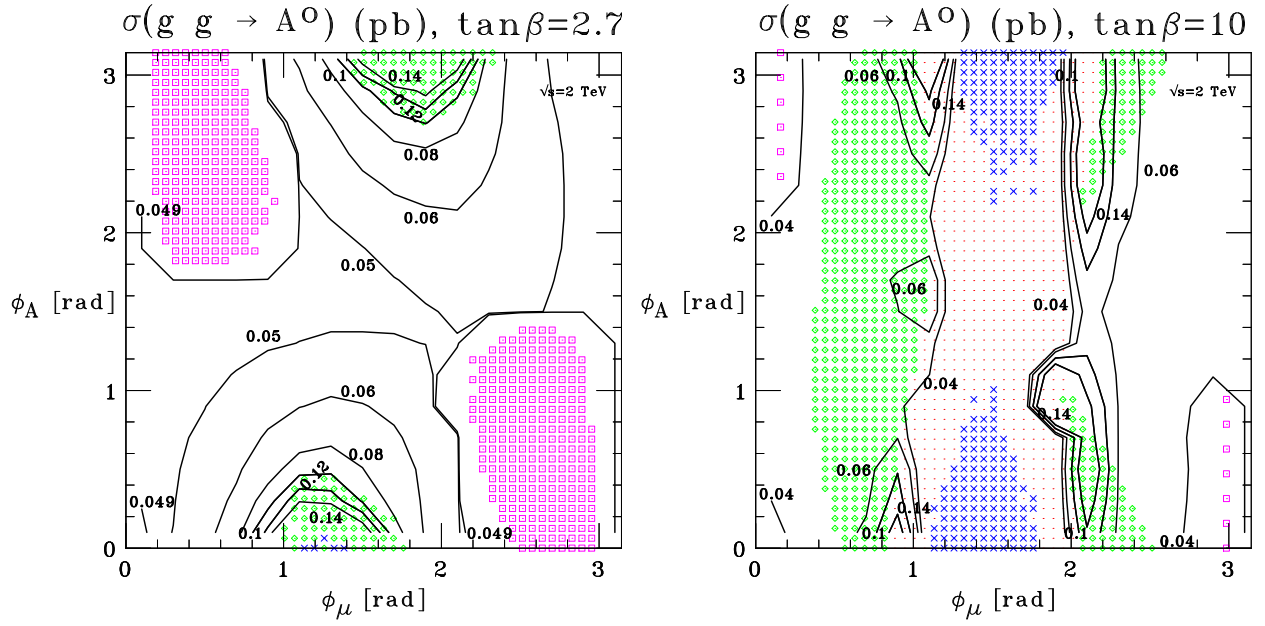


Figure 14: Same as in Fig. 12 for the case $A^0 = A^0$.